# TRABAJO ESPECIAL DE GRADO

# USO DE LOS RECEPTORES MLSE EN LAS COMUNICACIONES ÓPTICAS

Tutor Académico: Ing. Paolo Maragno

Presentado ante la Ilustre
Universidad Central de Venezuela
Por la Br. Roffé J., Eugenia
para optar al Título de
Ingeniero Electricista

Caracas, 2008

**Roffé J., Eugenia**

# USO DE LOS RECEPTORES MLSE EN LAS COMUNICACIONES ÓPTICAS

**Tutor Académico: Paolo Maragno. Tesis. Caracas. U.C.V. Facultad de Ingeniería. Escuela de Ingeniería Eléctrica. Ingeniero Electricista. Opción: Comunicaciones. 2007. 87 h.**

**Palabras Claves:** Fibra Óptica; Ecualización; MLSE; Interferencia Intersimbólica, Dispersión, Efectos no Lineales.

**Resumen.** Se estudia el uso de un ecualizador MLSE (Maximum-likelihood sequence-estimation) como solución a los problemas producidos por el aumento de la dispersión cromática que ocurre al aumentar el bit-rate de 2.5 Gbit/s a 10 Gbit/s en los sistemas de comunicaciones ópticas metropolitanos, y lograr de esta forma reutilizar la fibra que ha sido ya instalada. Se estudian las prestaciones de un ecualizador MLSE en un sistema de comunicaciones compuesto por un solo span de fibra, sin amplificación. Se analiza la efectividad de un receptor MLSE con 32 estados basado en el algoritmo de Viterbi en el caso en que la transmisión es afectada sólo por la dispersión cromática y en el caso en el que es afectada por la dispersión cromática y por los efectos no lineales para varios formatos de modulación binarios: intensity modulation direct detection (IMDD), duobinary (DB) y differential phase shift keying (DPSK). La modulación de varios niveles differential quadrature phase shift keying (DQPSK) también es analizada utilizando un procesador MLSE que toma decisiones conjuntas sobre los 2 bits que forman un símbolo.

POLITECNICO DI TORINO

Facoltà di Ingegneria dell’Informazione

Corso di Laurea in Ingegneria delle Telecomunicazioni

Tesi di Laurea

# Use of MLSE receivers in optical communications


Relatori:

Prof. Vittorio Curri

Prof. Gabriella Bosco

Candidato:

Eugenia Roffé


Novembre 2007

*To my mother, my father, my grandmother and my uncle*

# Acknowledgments

I wish to express my deepest gratitude to my supervisors Prof. Vittorio Curri and Prof. Gabriella Bosco for their guidance, suggestions and encouragement throughout the research.

I would like to thank FIDETEL, for supporting me financially these two years, and making my stay in Italy possible.

And finally, I would like to thank my parents and friends, who endured this long process with me, always offering support and love.

# Contents

# List of figures

# Acronyms

ACS: Add, Compare and Select

ASE: Amplified Spontaneous Emission

BER: Bit Error Probability

DB: Duobinary

DCF: Dispersion Compensating Fiber

DFE: Decision Feedback Equalization

DPSK: Differential Phase Shift Keying

DQPSK: Differential Quadrature Phase Shift Keying

EDC: Electronic Dispersion Compensation

FEC: Forward Error Correction

FFE: Feed-Forward Equalizer

FWM: Four Wave Mixing

IMDD: Intensity-Modulation Direct Detection

ISI: Intersymbolic Interference

Laser: Light Amplification by Stimulated Emission of Radiation

Led: Light Emitting Diode

MLSE: Maximum Likelihood Sequence Estimation

NRZ: Non Return to Zero

NZ-DSF: Non-Zero Dispersion Shifted Fiber

PMD: Polarization Mode Dispersion

OSNR: Optical Signal Noise Ratio

RZ: Return to Zero

SMF: Single Mode Fiber

SPM: Self Phase Modulation

XPM: Cross Phase Modulation

ZDP: Zero Dispersion Point

# Introduction

In the last years, the need to increase the velocity of transmission in optical communication systems, for example from 2.5 Gbit/s to 10 Gbit/s in metro area networks, has become evident. At this time, the big driver for upgrading to faster systems is the expected forthcoming video on demand (VOD) and Internet Protocol TV (IPTV) glut.

However, if the bit-rate is increased, the action of chromatic dispersion also increases, and intersymbol interference (ISI) produced by it degrades the system's performance.

It is then necessary to develop and use techniques which can control the increase of the ISI produced by the upgrading of the bit-rate. These techniques may be implemented in the transmitter or in the receiver without ever touching the transmission channel, in such way, the fiber already installed may be used again and new excavations which have a rather high cost may not be necessary.

To beat the various dispersion problems, modulation methods like Differential Phase-Shift Keying (DPSK), Differential Quadrature Phase-Shift Keying (DQPSK) and Duobinary (DB) are being tested and adopted. Further experimentation with alternative modulation methods can be expected as the push toward 40 Gbit/s and 100 Gbit/s systems progresses.

However, the most promising solution to overcome the dispersion problem is the use of some kind of Electronic Dispersion Compensation (EDC) in the receiver. EDC has garnered much attention and interest recently because of it potential to correct signal distortion in the electrical domain after detection with a photodetector.

One of the most promising technologies of EDC is the Maximum Likelihood Sequence Estimation (MLSE) approach, which has significant performance advantages over other algorithms such as Feed Forward Equalization (FFE) and Decision Feedback Equalization (DFE). The MLSE instead of using a decision circuit which makes bit-by-bit decisions based on a fixed threshold level, operates on bit sequences. The MLSE selects the most probable sent bit sequence conditional to the received sequence.

This technology is compatible with installed systems and works independently of any other receiver functions, such as FEC. In this way, the MLSE allows installed fiber to be immediately upgraded to support higher bit-rates without field plant purchases and deployment costs. Thus, service providers can save costs.

The aim of this thesis is to further investigate the performance of optical systems using both alternative modulation formats and a MLSE receiver.

This work is structured in six chapters. In the first chapter, an introduction to optical communications is presented; also a short history of such topic and a rough explanation of the structure of a generic communication system are discussed. In the second chapter, the modulation schemes which are being studied are explained: IMDD, DB, DPSK and DQPSK. In the third chapter, linear and non-linear effects of propagation in the fiber are discussed. In the fourth chapter, the functioning of MLSE is explained and also the algorithm upon which it is based, the Viterbi algorithm, is discussed. Finally, in the fifth and sixth chapter the results of the study which has been carried out using a purely dispersive fiber and a standard single mode fiber respectively are shown and analyzed.

# Chapter 1

# Introduction to optical communications systems

In the last years, optical fiber transmission systems have assumed a predominant position in the realm of high capacity long distance telecommunications.

The success that optical communications have achieved is due largely to the extraordinary transmission characteristics of the fiber:

- The fiber is the only transmission medium allowing an enormous bandwidth (potentially 25 THz).
- Also, it allows reaching long distances due to its low attenuation.
- It is also immune to electromagnetic disturbances since it does not use conductors and the disturbances generated by the fiber itself are nil. This characteristic and the fact that fibers have very reduced dimensions allow the grouping of a large number of fibers in a cable.

Today, the optical fiber, thanks to the aforementioned characteristics, is an irreplaceable transmission medium in many fields of digital communications.

In this chapter, the historical evolution of optical communications systems will be presented and the basic structure of a generic optical system will be explained.

## 1.1 A brief history of fiber optics technology

The first communication system using light was created in the 1790's by the French Chappe brothers who invented the "optical telegraph". This was a system comprised of a series of lights mounted on towers where operators would relay a message from one tower to the next.

On the other hand, the guided propagation of light began to be studied in the XIX century, when in the 1840's physicists Daniel Collodon and Jacques Babinet showed that light could be directed along jets of water. Then in 1870 physicist John Tyndall demonstrated that light followed a zigzag path inside a curved path of water thereby proving that a light signal could be bent.

The first applications of guided light propagation began at the end of the XIX century, when in 1888 doctors in Austria used bent glass rods to illuminate body cavities.

It was not until the XXth century that guided light propagation was used for communications and significant improvements were made to this technology. Fiber optic technology experienced a phenomenal rate of progress in the second half of the XXth century.

Early success came in the 1950's with the development of the fiberscope, which was an image transmitting device that used the first practical all-glass fiber. However early all-glass fibers experienced excessive optical loss as the signal traveled the fiber, limiting transmission systems.

This motivated scientists to develop glass fibers that included a separate glass coating. The innermost region of the fiber, the core, was used to transmit the light, while the glass coating, the cladding, by having a lower refractive index than the core, prevented the light from leaking out of the core by reflecting the light within its boundaries.

The development of laser technology was the next important step in the establishment of the industry of fiber optics. Laser went through several generations, including the development of the ruby laser and the helium-neon laser in 1960. Semiconductor lasers, which are widely used in fiber optics today, were first developed in 1962.

Because of their higher modulation frequency capability, the importance of lasers as a means of carrying information did not go unnoticed by communications engineers. However, the laser is unsuited for air transmission since it is adversely affected by environmental conditions such as rain, snow and smog. Faced with the challenge of finding a transmission medium other than the air, in 1966 it was proposed that optical fiber might be a suitable transmission medium if its attenuation could be kept under 20 dB/Km. At the time of this proposal, optical fiber exhibited losses of 1000 dB/Km or more. Intuitively, researchers proposed that the high optical losses were the result of impurities in the glass and not the glass itself.

So, glass researchers began to work on the problem of purifying glass, and in 1970 succeeded in developing a glass fiber that exhibited attenuation smaller than 20 dB/Km, the threshold for making fiber optics a viable technology.

The early work on fiber optic light source and detector was slow and often had to borrow technology developed for other reasons. For example, the first optical fiber light sources were derived from visible indicators LEDs. But as demand grew, light sources that offered higher switching speed, more appropriate wavelengths and higher output power were developed.

Fiber optics developed over the years in a series of generations that can be closely tied to wavelengths.

The earliest fiber optic systems were developed at an operating wavelength of about 850 nm. This wavelength corresponds to the so called *first window* in a silica-based optical fiber. This window refers to a wavelength region that offers low optical loss. It sits between large absorption peaks caused primarily by moisture in the fiber and Rayleigh scattering.

The 850 nm region was initially attractive because the technology of light emitters at this wavelength had already been perfected in visible indicator LEDs and low cost silicon detectors could also be used. As technology progressed, the *first window* became less attractive because of its relatively high 3 dB/Km loss limit.

Then, most companies jumped to the *second window* at 1310 nm with lower attenuation of about 0.5 dB/Km.

And in 1977 the *third window* at 1550 nm was developed. This window offered the theoretical minimum optical loss for silica-based fibers, about 0.2 dB/Km [1].

In the 80's, the multimodal fibers were substituted by single mode fibers and the first optical amplifiers using fiber doped with erbium, the *Erbium Doped Fiber Amplifier* (EDFA), were developed.

In the 90's the technique of *Wavelength Division Multiplexing* (WDM) is introduced. Also the definite success of optical communications was established with the development of new types of fibers and of optical integrated components which allowed a constant and rapid increase in optical communications.

Among the most significant areas of research in the last ten years we may quote the study of new modulation formats, compensation of dispersion and the Raman amplification.

The tendency in recent research is to accomplish the implementation of most of the functions of a network in the optical domain.

## 1.2 A generic optical communications system

The main components which form an optical system are: the transmitter, the communication channel which is the optical fiber and the receiver. The system can be schematized in a very simple way in Figure 1.1.

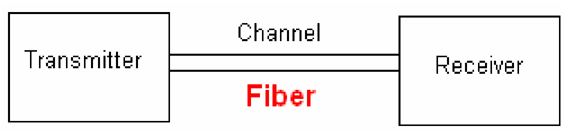


Figure 1.1. Generic optical transmission system

The preceding scheme does not differ much from any communication system, the main difference lies in the communication channel which is the optical fiber and consequently, the transmitter and the receiver must be designed to work with this type of channel.

## 1.2.1 The optical transmitter

The function of the optical transmitter is to convert an electrical signal applied to its entry into an optical signal which may be transmitted on to the fiber.

There are two different types of transmitter: one that uses *direct modulation* and one that uses *external modulation*.

- *Transmitter with direct modulation*

  The transmitter which uses direct modulation is represented in Figure 1.2.

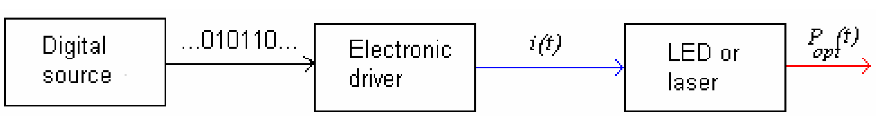


Figure 1.2. Transmitter using direct modulation

When using direct modulation, the laser is guided between two different current levels to represent “0” and “1” so the signal comes out of it already modulated in intensity as is shown in Figure 1.3.

This modulation is easy to implement, but it has the disadvantage that a variation in the current which enters the laser causes a variation in the frequency and phase of the output signal. This causes the modulated signal to occupy a wide bandwidth and the effect of chromatic dispersion is increased.

This type of modulation is used for transmissions under 2.5 Gbit/s and under 40 or 50 Km, and to transmit just one channel.

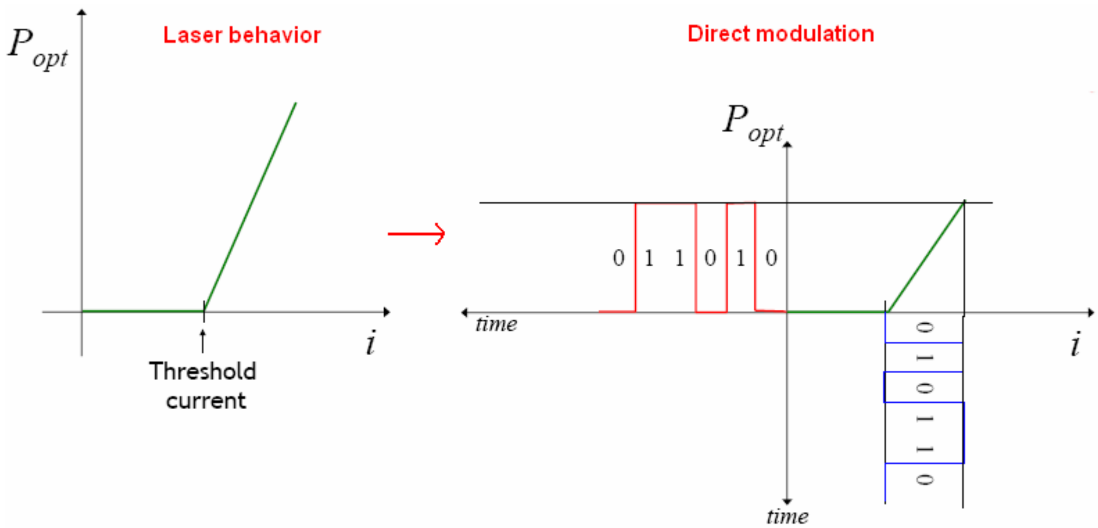


Figure 1.3. Direct modulation

- *Transmitter with external modulation*

The transmitter using external modulation is represented in Figure 1.4.

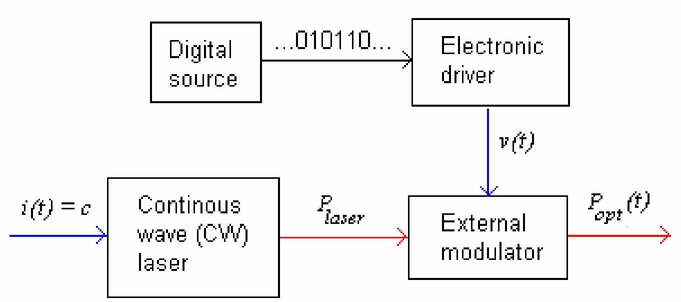


Figure 1.4. Transmitter using external modulation

When using external modulation, the laser is used only as a source of optical power and is kept at constant current. This causes a very stable output power with a narrow spectrum.

To apply the modulation, an external modulator which modulates the intensity, phase or polarization of the constant power output of the laser is used.

The external modulation generates a narrower band signal than the direct modulation, and it yields better results regarding chromatic dispersion, but yet, it is more costly.

This type of modulation is used for long distance transmissions and in DWDM systems.

Any type of transmitter is based on the use of an optical source. Optical sources are active devices which emit electromagnetic radiation at the optical frequencies. These can be classified in *Light Emitting Diodes* (LED) and *Light Amplification by the Stimulated Emission of Radiation* (LASER)

- *LED*

The LED works thanks to the phenomenon of *spontaneous emission*. In the spontaneous emission, as is represented in Figure 1.5, an electron drops spontaneously from the high energy level $E_2$ to the low energy level $E_1$ and as a consequence a photon with energy $E_2$-$E_1$ is generated contemporarily. The frequency of the generated photon is determined by Planck's law:

$$h \cdot f_{photon} = E_2 - E_1 \quad (1.1)$$

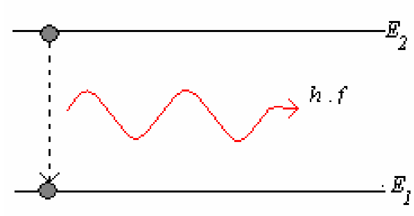


Figure 1.5. Spontaneous Emission

In the LED photons are generated in a random manner in every direction and in an ample range of frequencies, but only a fraction of photons emitted couple on to the fiber.

As a first approximation the optic output power is proportional to the injected current.

$$P_{out} = k \cdot I(t) \tag{1.2}$$

The LED has a low output power, a low modulation velocity and its use in optical systems brings strong limitations caused by dispersion due to the fact that the output signal bandwidth is wide. Consequently, this are used in low cost applications, tipically with multimode fibers, in short distances (1 Km maximum) and low bit-rates (up to 155 Mbit/s).

- *LASER*

In a semiconductor laser, photons are generated in a p-n junction polarized directly. Then, these photons are forced to transit in the inner structure several times by using some type of partially reflector filter placed on both its sides. During transit, the photons are amplified by the effect of the *stimulated emission*.

In the stimulated emission, an electron drops from the conduction band to the valence band due to the interaction with an incoming photon, and consequently a photon with the same frequency and phase of the incoming one is generated, that is to say, it is coherent with it. This phenomenon is represented in Figure 1.7.

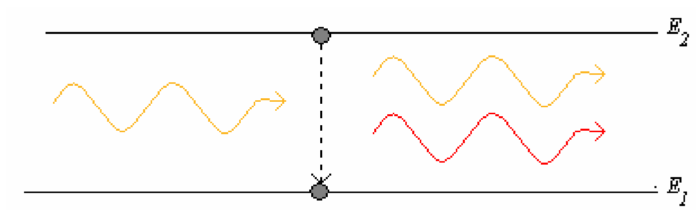


Figure 1.7. Stimulated Emission

There are different laser technologies, but all of them allow us to transmit at a larger distance and with a higher modulation speed than the LED, and also the signal they produce has a narrower spectrum so that tolerance to chromatic dispersion increases. Thus, the laser is used as an optical source is systems which require better performance.

## 1.2.2 The optical fiber

The optical fiber is a dielectric waveguide with a cylindrical geometry which is made with highly pure silica. In the fiber's structure two sections can be recognized: the inner part which is where the light travels called *core* and the outer part called *cladding* which has a refractive index lower than the core. This structure may be observed in Figure 1.8.

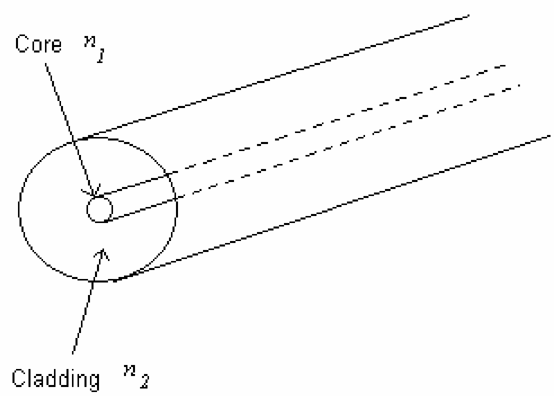


Figure 1.8. Optical fiber

The functioning principle of the fiber is based in what happens when a ray of light strikes a boundary between two different materials. As is observed in Figure 1.9, when a ray of light strikes the boundary between two mediums which have different refractive indexes ($n_1$>$n_2$) this is partly reflected and partly transmitted according to Snell's law:

$$n_1 \sin(\alpha) = n_2 \sin(\beta) \qquad (1.3)$$

where α is the angle of incidence with respect to the normal to the surface and β is the angle that the transmitted ray forms with this normal.

The angle β increases when α increases up to the limit value of β=π/2, at which there is no transmitted ray. This is the phenomenon of *total reflection*, and the *critical angle* is the angle of incidence above which the total reflection occurs, this angle is represented as:

$$\alpha_L = \arcsin\left(\frac{n_2}{n_1}\right) \qquad (1.4)$$

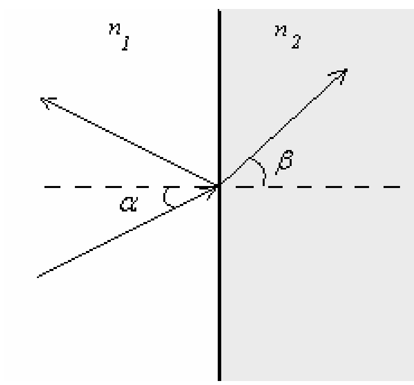


Figure 1.9. Incidence of a ray of light at a boundary between two mediums

The light transmission in the inner part of the fiber is based on the phenomenon of total reflection, which is produced when the ray strikes the surface between the core and the cladding. The concept of *fiber acceptance angle* is then introduced: all angles smaller than the acceptance angle are guided (this is to say, they have total reflection). The fiber acceptance angle is represented as:

$$\theta = \sqrt{\frac{n_2^2 - n_1^2}{n_0}} \qquad (1.5)$$

where $n_0$ is the refractive index of the medium external to the fiber.

The light rays which enter with an incidence angle larger than the acceptance angle will strike the surface between the core and the cladding with an angle smaller than the critical angle and a part will be transmitted to the cladding not allowing for total reflection. This phenomenon is shown in Figure 1.10.

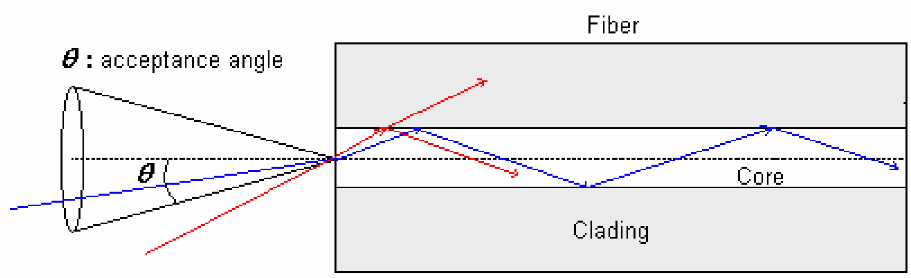


Figure 1.10. Cone of acceptance

There are two basic types of fiber: multimode fiber and single mode fiber [2]:

- *Multimode fiber*

  This fiber was the first to be manufactured and commercialized, and its denomination simply refers to the fact that numerous light rays (modes) are carried simultaneously through the fiber. Modes result from the fact that light will only propagate in the fiber core at discrete angles within the cone of acceptance. This fiber type has a much larger core diameter compared to the single mode fiber and is easiest to couple to other components.

  Multimode fiber is best designed for short transmission distances, and is suited for use in low cost LAN systems.

- *Single mode fiber*

  In the single mode fiber just one mode is carried along the fiber's axis. Single mode fiber allows for a higher capacity to transmit information because it can retain the fidelity of each light pulse over longer distances, and it exhibits no dispersion caused by multiple modes. Single mode fiber also enjoys lower attenuation than multimode fiber.

Single mode fiber is best designed for longer transmission distances, making it suitable for long distance telephony and multichannel television broadcast systems, and, in general, high capacity data transmission.

Single mode fiber has gone through a continuing evolution for several decades now. As a result, there are three basic classes of single mode fiber used in modern telecommunications systems:

- *Standard single mode fiber* (SMF)

  Is the oldest and most widely deployed type. These fibers were initially intended for use near 1310 nm, and later the 1550 nm systems made these fibers less desirable due to their very high dispersion at this wavelength.

- *Dispersion shifted fiber* (DSF)

  To address the problem of the high dispersion at 1550 nm of the SMF, manufactures developed the DSF, which moved the zero dispersion point to the 1550 nm region.

- *Non zero dispersion shifted fiber* (NZ-DSF)

  Years later, scientists would discover that while DSF worked extremely well with a single 1550 nm wavelength, it exhibits serious non linearity impairments when multiple, close-spaced wavelengths in the 1550 nm region were transmitted in DWDM systems. To address this shortcoming, the NZ-DSF was introduced. Some of the non-linear effects affect the system mainly when chromatic dispersion is low. The NZ-DSF presents a highly enough dispersion as to reduce the impact of its non-linear effects, and at the same time low enough as to limit the linear distortion of the signal.

### 1.2.3 The optical receiver

The last block is formed by the optical receiver. This has the function of converting the optical received signal in an electrical signal, and, when observing this signal in a one bit period it must determine which of the two possible bits “0” or “1” was transmitted.

Generally, the receiver is formed by: an optical filter, a photodiode and an electric receiver.

The optical filter has the functions of extracting a desired wavelength from the WDM comb and of cuting out the noise introduced by amplifiers and interference of adjacent channels.

The photodiode has the function of converting the received optical power into an electric current which later will enter the electric receiver.

In the electric receiver, the decisions about the received bits are taken. The process of incoherent demodulation called *Direct Detection* is in principle very simple: the receiver detects the presence or absence of optical power in the bit slot. In order to guarantee that the sampling instant be the closest to the optimal instant, which corresponds to the instant of larger aperture of the eye diagram, a circuit is necessary to recover synchronism. Yet, in the case of coherent demodulation, a circuit which nears phase recovery is necessary.

In the signal reception procedure errors are obviously produced, because the signal is affected by phenomena which impair the system’s performance (for instance ASE noise, the shot noise, the thermal noise, the distortion due to non linear effects and the ISI). These phenomena must be taken into account in the system’s design phase so that a given *Bit Error Rate* (BER) may be reached.

Among the parameters which describe the system’s performance we may recognized: the BER (which is typically $1.10^{-12}$ for high speed optic systems), the Q factor, which is a sort of signal-to-noise ratio, and the sensitivity, which is the receiver power necessary to obtain a prefixed BER.

# Chapter 2

# Optical modulation formats

Modulation is the process by which digital information is converted into an optical format which may be sent through the fiber.

There is a great variety of modulation formats and in the optical realm these may be grouped into two large categories: direct modulation of the optical source (which may only be an amplitude modulation) and external modulation (which may be an amplitude modulation, a phase modulation or a polarization modulation).

Most currently deployed optical fiber communication systems exploit IMDD to transmit information, which is a technique simple to implement, but places several limits on information capacity. A further improvement in system performance can be achieved looking to alternative modulation formats. Encoding information on the phase, for example, enables constant intensity, which is preferable in optical fiber transmission, but requires more complex coherent receivers.

In this chapter four different digital modulation techniques are presented, these are: *Intensity Modulation Direct Detection* (IMDD), *Duobinary* (DB), *Differential Phase-Shift Keying* (DPSK) and *Differential Quadrature Phase-Shift Keying* (DQPSK).

# 2.1 IMDD

Since their introduction, optical communications have been based on the easiest modulation format: IMDD.

In this format, information is coded on the intensity of the optical signal: if a bit slot contains power, that bit is a "1", and if it does not contain power then the bit is a "0".

The simplest way to implement such format is to switch on and off the optical source, which corresponds to the direct modulation of the laser. This was the base for a first generation of optical systems.

Later, in order to enhance the system's performance, external modulation was introduced. In this type of modulation, the laser is kept at a constant current giving place to a very stable output power which is later modulated with an external modulator as is shown in Figure 2.1.

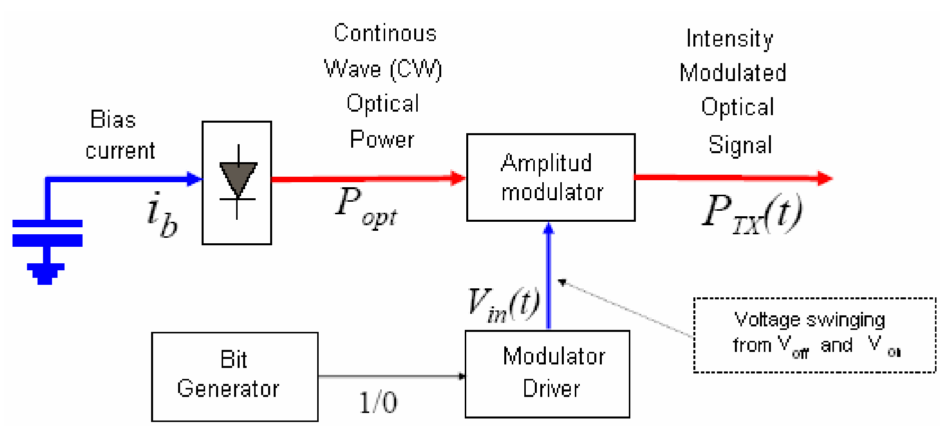


Figure 2.1. IMDD transmitter with external modulation

The most used modulator is the *$LiNbO_3$ Mach-Zehnder modulator*. The basic structure of this modulator comprises two waveguides, two Y-junctions and a RF/DC electrode. The optical signals launched into the modulator are equally split into two waveguides at the first Y-junction on the substrate. When voltage is not applied to the RF electrode, the two signals are recombined at the second Y-junction in phase and coupled into a single output. In this case the output signal is recognized as a “1”. When voltage is applied to the RF electrode, the refractive index is changed due to electro-optic effects and the phase of the signal in one arm is advanced and the phase of the signal in the other arm is retarded, and when the two signal are recombined at the second Y-function they are lost. In this case the output signal is recognized as a “0”. The voltage difference which induces the “0” and the “1” is called driving voltage, and is an important parameter when designing the modulator.

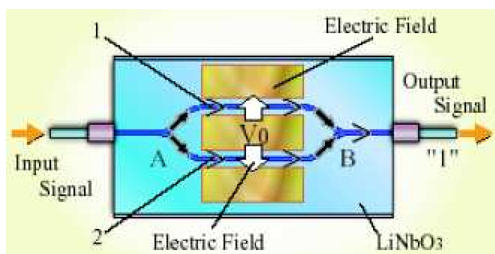


Figure 2.2. Mach-Zehnder modulator

Intensity modulation may be carried on with two types of coding which are differentiated according to the type of pulse used for transmission. The RZ (*Return to Zero*) coding uses a pulse that returns to zero within the bit slot, and the NRZ (*Non Return to Zero*) coding uses pulses that have the same duration as the bit slot. In Figure 2.3 a sequence o bits using the two codings is shown.

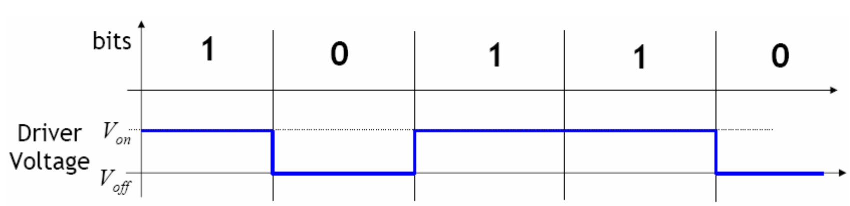

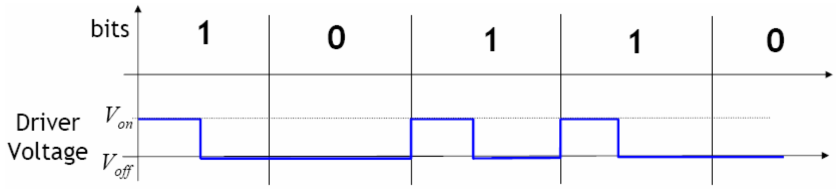


Figure 2.3. (a) NRZ encoding (b) RZ encoding

NRZ modulation has the advantage of having an easy implementation and of having a small spectral occupancy (favouring the presence of many channels) and is practically the standard of optical communications. But it has the disadvantages of the high impact that the non-linearities of the fiber have over it.

RZ modulation, on the other hand, has the advantage of the very little effect non-linearities of the fiber have upon it. But it has the disadvantage of ample spectral occupancy and more complicated implementation.

For all modulation formats based on Intensity Modulation the receiver set-up is like the one shown in Figure 2.4.

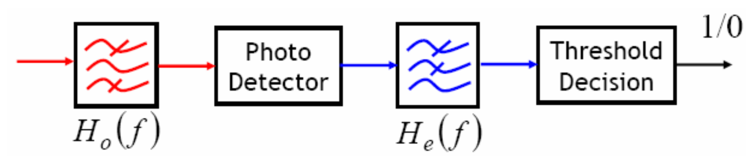


Figure 2.4. Typical IM receiver

## 2.2 Duobinary

Duobinary is a modulation based on line-coding, in which the sequence is manipulated in different ways before being sent on to the fiber. With this modulation scheme, the signal transmitted at a certain time depends on both the bit at that time and on one or more of the previous bits. Is a scheme that has very good spectral efficiency as it transmits R bits/s using less than R/2 Hz of bandwidth.

Nyquist's result says that in order to transmit R bits/s with no intersymbol interference, the minimum bandwidth required of the transmitted pulse is R/2 Hz. This result implies that duobinary pulses will have ISI. However, this ISI is introduced in a controlled manner so that it can be subtracted out to recover the original values.

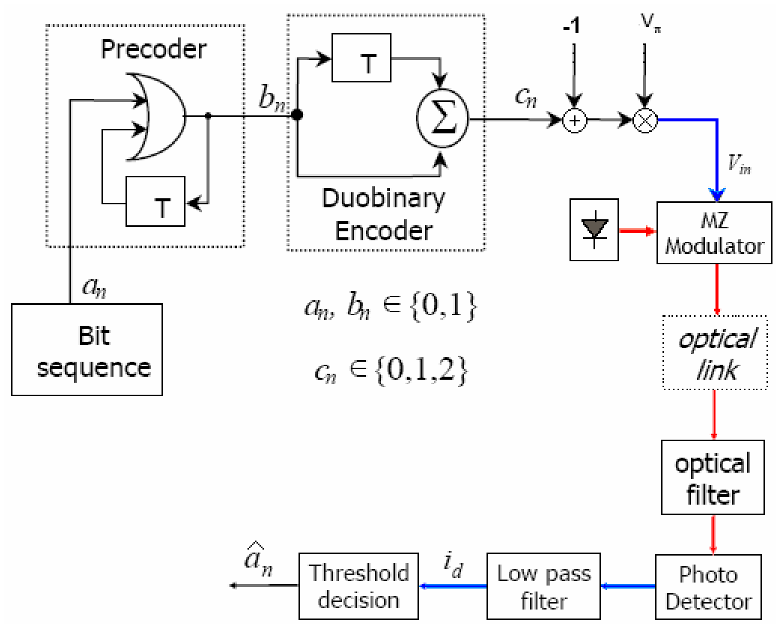


Figure 2.5. Duobinary squeme

The scheme of the Duobinary modulation is shown in Figure 2.5. As it may be seen, the data sequence goes in the first place through the *precoder*, where a XOR logic operation takes place between the current bit and the previous output bit from the precoder. The precoder output then enters into the *encoder* where the addition of the current bit and the preceding bit takes place, thus generating a signal which has three levels "0", "1" and "2". After the encoder, a -1 is added so that the signal is symmetric in relation to level "0". As a result, the signal shown in Figure 2.6 is obtained. At this point, the signal is multiplied by $V_\pi$ and then it controls a Mach-Zehnder modulator.

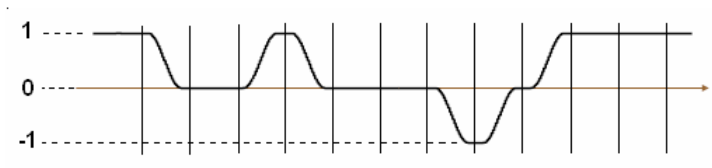


Figure 2.6. Duobinary three level signal

The duobinary receiver is a conventional single-photodiode receiver that looks at power, converting again the three leveled signal into a two level signal, as it is seen in Figure 2.7.

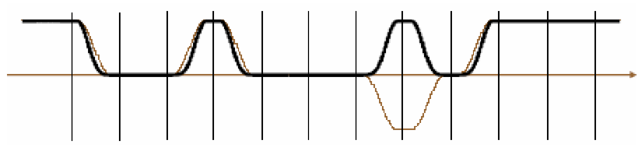

Figure 2.7. Duobinary two level signal

## 2.3 Optical phase modulations

For optical communications the use of phase modulation is an interesting opportunity. There are two fundamental ways of using the phase of a signal to represent a data sequence:

- By detecting the phase itself as conveying the information in which case is necessary a coherent demodulator, that must have a reference signal to compare the received signal's phase against; or
- By detecting the *change* in the phase as conveying information. These are called *differential* schemes and they do not need a reference carrier.

In the first case, there is an ambiguity of phase if the constellation is rotated by some effect in the communications channel. This problem can be overcome by using the data to change the phase rather than set the phase; this is to say, using a differential modulation format.

There are two kinds of differential phase modulation schemes: the *Differential Phase Shift-Keying* (DPSK) and the *Differential Quadrature Phase-Shift Keying* (DQPSK).

## 2.3.1 DPSK

In this modulation scheme a binary "1" may be transmitted by adding 180° to the current phase and a binary "0" by adding 0° to the current phase. A modulated signal is shown in the Figure 2.8. It is assumed that the signal starts with *zero phase* and there is a phase shift at $t$=0.

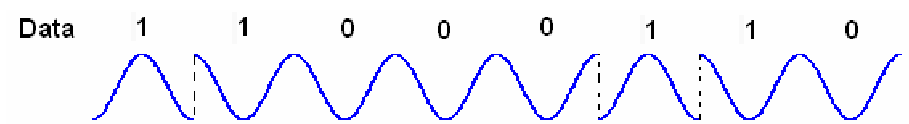


Figure 2.8. Modulated DPSK signal

A DPSK modulation may be generated in two different ways. An intensity modulator or a phase modulator as shown in Figure 2.9 may be used. Using a phase modulator, the information is transferred within the signal's phase (while amplitude remains constant), controlling the modulator with a tension in the interval $0/V_{\pi}$. Using, on the other hand, an intensity modulator, this is controlled with a tension in the interval $-V_{\pi}/V_{\pi}$.

In the differential precoder the XOR operation is performed between the transmitted bit and the precoder's previous output bit. The precoder is shown in Figure 2.10.

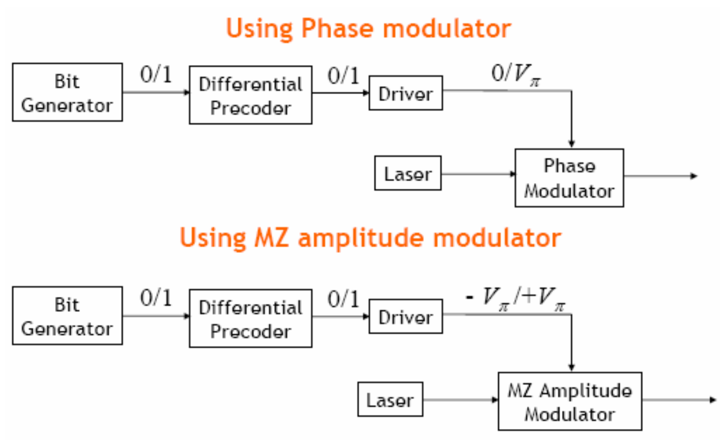


Figure 2.9. DPSK transmitters

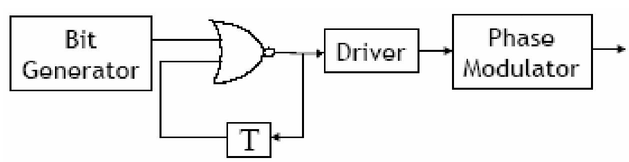


Figure 2.10. DPSK precoder

The DPSK receiver is shown in Figure 2.11. The receiver consists of an *Asymmetric Mach-Zehnder Interferometer*, which delays one bit in one arm so two bits can be compared at the same time, and a *balanced photo detector*, which should be perfectly balanced (have identical responsivity) in order to avoid problems. In principle, the DPSK can be detected using only one photodiode on either output, but the two ports form slightly different signals which produce different "eyes" and the balanced photo detector sums the "eyes" reinforcing each other.

It is important to point out that the DPSK reduces the impact of the fiber non linearities and avoids coherent reception, but it needs a precoder in the transmitter side and an asymmetric interferometer and an expensive balanced photo detector at the receiver.

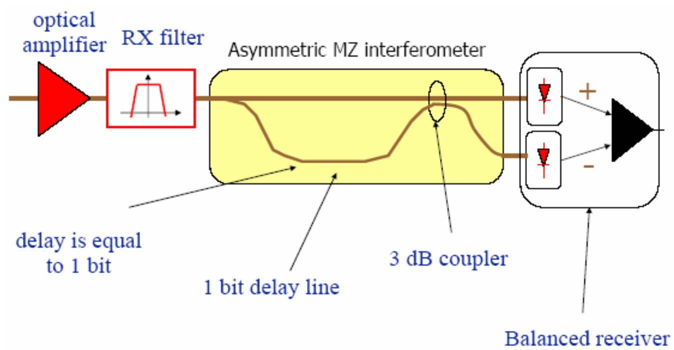


Figure 2.11. DPSK receiver

## 2.3.2 DQPSK

This scheme is a 4-level differential phase modulation. With a “conventional” binary modulation scheme, the transmitter has to emit as many pulses per second as the bit rate, but with a 4-signal scheme that ratio is halved. This halves the spectral width and therefore the bandwidth efficiency greatly increases.

In this modulation scheme the phase shifts are 0°, 90°, 180° and -90° which may correspond to the four symbols “00”, “01”, “11” and “10”. A modulated signal is shown in the Figure 2.12. It is assumed that the signal starts with *zero phase* and there is a phase shift at $t$=0.

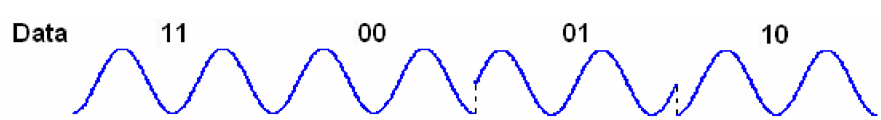


Figure 2.12. Modulated DQPSK signal

The precoder is much more complex than for DPSK, and is shown in Figure 2.13.

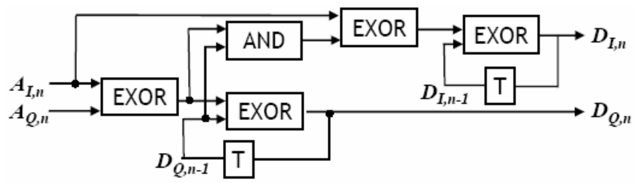


Figure 2.13. DQPSK precoder

The DQPSK transmitter and receiver are shown in Figures 2.14 and 2.15 respectively. It is seen that the receiver consists of two DPSK receivers.

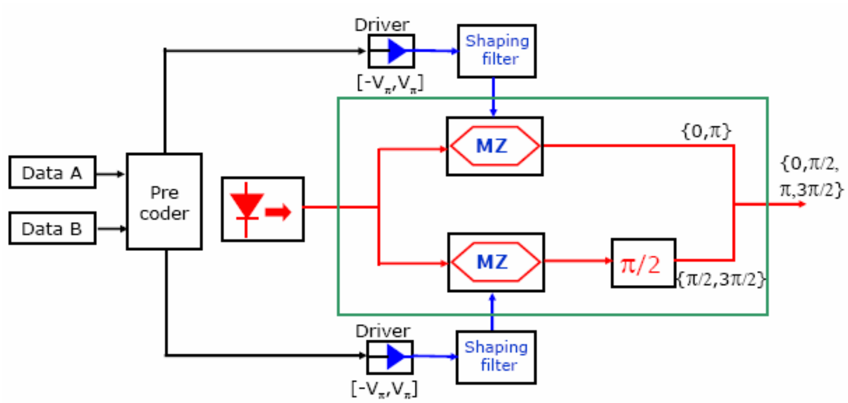


Figure 2.14. DQPSK transmitter

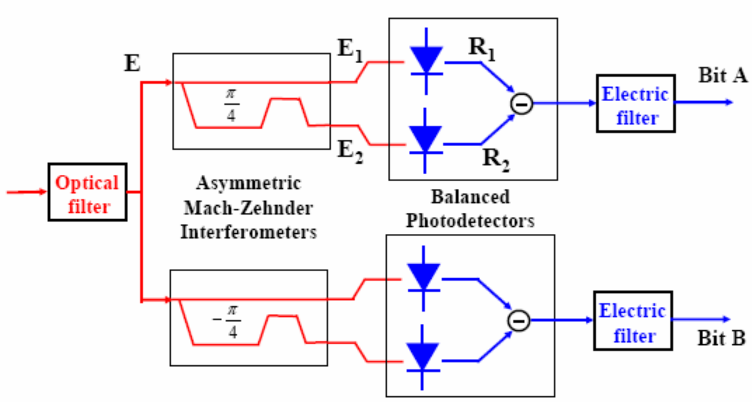


Figure 2.15. DQPSK receiver

It is important to point out that the DQPSK modulation format has the advantages of having reduced bandwidth requirements and of increasing the tolerance to chromatic dispersion and fiber non linearities, but it needs a complex precoder at the transmitter side, and two asymmetric interferometers and two expensive balanced photodetectors at the receiver.

# Chapter 3

# Optical fiber propagation effects

In an optical transmission system, when the signal propagates through the fiber, linear and non linear propagative phenomena are manifested. The linear effects may be modeled by a transfer function which is independent of the input signal; but the non linear effects depend on the input signal and cannot be modeled by a transfer function.

## 3.1 Linear effects

Considering the propagation of the optical field through a single mode fiber, and neglecting the non linear effects for now, the evolution of the amplitude along the propagation coordinate *z* is given by the wave equation:

$$\frac{\partial E}{\partial z} = -\alpha(\omega)E - j\beta(\omega)E \tag{3.1}$$

where $\alpha(\omega)$ is the attenuation constant and $\beta(\omega)$ is the propagation constant.
This equation admits the analytic solution:

$$E(\omega, z) = E(\omega,0)e^{-\alpha(\omega)z}e^{-j\beta(\omega)z} = E(\omega,0)H_F(\omega, z) \tag{3.2}$$

where $H_F(\omega)$ is the fiber's transfer function.

In the following, the attenuation and the dependence of the propagation constant on the frequency, which generates the chromatic dispersion, will be analyzed separately.

### 3.1.1 Attenuation

The attenuation introduced by a fiber span is defined by the ratio between the power at the beginning of the fiber and the received power.

When a signal propagates through the fiber, part of its energy is absorbed by the material, which generates a loss in the signal power.

The attenuation is caused by phenomena as the Rayleigh scattering and the infrared absorption, which depend on the material and are due to the presence of imperfections and impurities. The attenuation also depends on the wavelength, the type of fiber and the possible mechanical strains applied to the fiber.

As it can be seen in Figure 3.1 the attenuation has an absolute minimum of 0.2 dB/Km around 1550 nm, and a relative minimum of 0.4 dB/Km around 1300 nm. These wavelengths define the spectral windows in which the fiber is used.

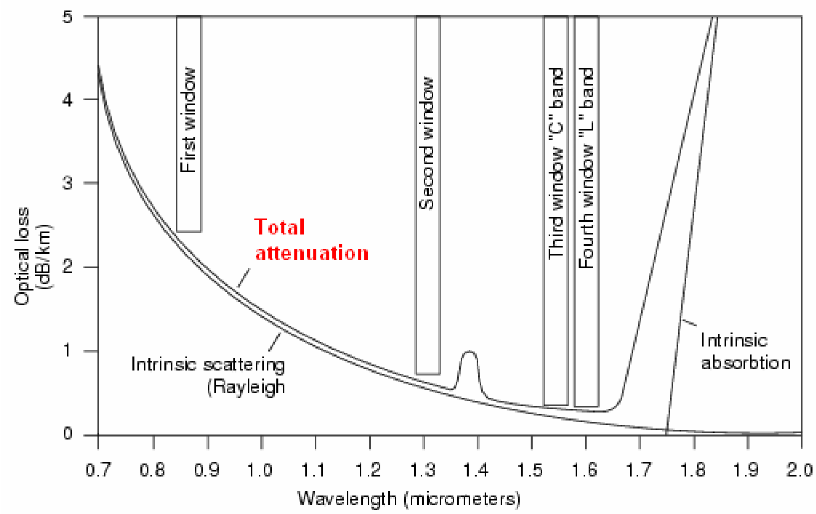


Figure 3.1. Attenuation of a single mode fiber

The attenuation can be considered constant in the bandwidth used for the transmission; thus the dependence of the attenuation on the wavelength can be neglected. So, under this hypothesis, the attenuation is a non distortional effect.

### 3.1.2 Chromatic dispersion

The propagation constant depends on the wavelength, meaning that the signal's different spectral components propagate with different velocities.

In consequence, the received signal is distorted. Pulses widen in time and interfere with adjacent pulses, so the eye diagram closes itself. This phenomenon is called Intersymbol Interference (ISI), which reduces the performance of the system. The dispersion limit, which is the maximum distance at which the system is still capable of working, decreases as the bit rate increases.

Dispersion has two contributions, the material dispersion and the waveguide dispersion. The material dispersion is caused by the dependence on the frequency of the material's refractive index. On the other hand, the solution of the propagation equation for the fundamental mode gives origin to a dependence of the group velocity on the frequency; this is the waveguide dispersion, this depends on the project parameters and can be controlled. The total chromatic dispersion is approximately the addition of these two, as shown in Figure 3.2.

The study of chromatic dispersion may be approached by developing Taylor's series of the propagation constant around the central frequency. We obtain:

$$\beta(\omega) \cong \beta_0 + \beta_1 \cdot (\omega - \omega_0) + \frac{\beta_2}{2} \cdot (\omega - \omega_0)^2 + \frac{\beta_3}{6} \cdot (\omega - \omega_0)^3 + \ldots \qquad (3.3)$$

with

$$\beta_i = \left( \frac{\partial}{\partial \omega} \right)^i \beta(\omega) \Big|_{\omega = \omega_0} \qquad (3.4)$$

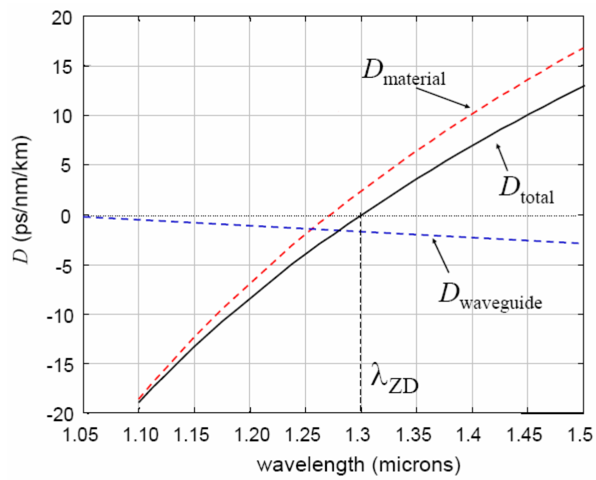


Figure 3.2. Total chromatic dispersion for G. 652 fiber

The term $\beta_0 = \beta(\omega_0)$, at a given distance *z*, determines a constant phase rotation which do not distort the impulse.

The term $\beta_1$ introduces a delay $\tau_g$, known as *group delay*, which is substantially the propagation delay of the pupulses:

$$\tau_g(\omega_0) = \beta_1 z = \left.\frac{\partial \beta}{\partial \omega}\right|_{\omega=\omega_0} z \tag{3.5}$$

This delay, proportional to *z*, is independent of the frequency, which means that also $\beta_1$ does not contribute to the distortion of the impulse.

The term $\beta_2$, on the other hand, causes a delay which depends on the frequency and is proportional to *z*.

Considering the contribute of $\beta_2$, the total delay is:

$$\tau_g(\omega) = \tau_g(\omega_0) + \beta_2 \cdot (\omega - \omega_0) \cdot z \tag{3.6}$$

where $\tau_g(\omega_0)$ represents an average group delay which is independent of the frequency, and the second term originated by $\beta_2$ is a delay which takes a different value for each spectral component of the transmitted pulse.

The constant $\beta_2$ may be positive or negative; then, two cases may be considered:

- *Normal Dispersion Regime*: This is the case in which $\beta_2$>0. In this case, spectral components with larger frequencies propagate with a lower velocity than the spectral components with smaller frequencies.
- *Anomalous Dispersion Regime*: This is the case in which $\beta_2$<0. In this case, the spectral components with larger frequencies propagate more rapidly.

Generally, the measure of dispersion in the optical fiber is expressed by means of parameter *D*, which is related to $\beta_2$ by the following relation:

$$D = \beta_2 \cdot \left( -\frac{2\pi c}{\lambda^2} \right) = -0.785 \cdot \beta_2 \quad \left[ \frac{ps}{nm \cdot Km} \right] \tag{3.7}$$

For example, at a wavelength of 1550 nm standard SMF fibers have $\beta_2 \cong$ -20 $ps^2$/Km and $D \cong 16$ ps/nm/Km, and so they operate in an anomalous dispersion regime.

The delay introduced by $\beta_3$ is also dependent on the frequency, and so it causes the distortion of the impulse waveform:

$$\tau_g \beta_3 = \frac{1}{2} \beta_3 \cdot (\omega - \omega_0)^2 \cdot z \tag{3.8}$$

But as $\beta_3$ takes very small values, its contribution may generally be neglected.

Chromatic dispersion is a phenomenon which may be compensated. There are several different techniques for compensating dispersion; these may be classified in optical and electronic compensation.

Optical compensation consists in introducing, after each fiber span, a particular fiber called *Dispersion Compensating Fiber* (DCF), which by having a dispersion *D* with opposite sign to the precedent fiber, cancels the phenomenon of dispersion achieving a value of accumulated dispersion theoretically equal to zero. Nevertheless, in the presence of non-linear phenomena, dispersion compensation is more complicated, and must be achieved by using dispersion maps obtained by means of numerical simulation.

On the other hand, electronic compensation is achieved through an equalizer place at the receiver. There are three principal architectures/algorithms: Maximum Likelihood Sequence Estimation (MLSE), Feed-Forward Equalizer (FFE) and Decision Feedback Equalizer (DFE). The first one uses purely digital techniques, while the others are based on analog processing, which has proven difficult to be designed well.

- MLSE: This is the most recent and most advanced approach. It uses a Viterbi algorithm for equalization. Its adaptative digital performance is widely recognized as far superior when compared to the other analog approaches (FFE and DFE).
- FFE: This is the most basic scheme. It uses a FIR filter, several stages of delay, coefficient multiplication and addition to provide compensation. By approximating the inverse of the channel's transfer function, automatic control of coefficients can provide adaptative operation.
- DFE: This is an FFE with a second FIR added to form a feedback loop. The decision threshold of the data recovery circuit is shifted to compensate for the influence of past data levels and so provide improved performance compared with FFE.

The MLSE technique has been proved to yield very good results in optical transmission systems; this technique will be studied in detail in chapter 4.

### 3.1.3 Polarization mode dispersion (PMD)

In single mode fibers, two modes of the electromagnetic field polarized in orthogonal directions may be propagated. PMD is due to the difference in speed of these polarization modes. This difference in speed results from birefringence, a phenomenon where the refractive index differs from one input polarization state to another. Birefringence is caused by small defects in the manufacturing process, bends, and other mechanical stresses that may affect the circular fiber geometry [3].

The impact of PMD may generally be neglected in the transmissions at 10 Gbit/s, while it becomes a limiting factor at 40 Gbit/s.

## 3.2 Non linear effects

The quality and capacity of the transmission in the optical systems for long distances is certainly influenced by non-linear effects. These effects are: *Self Phase Modulation*, *Cross Phase Modulation* and *Four Wave Mixing*.

The physical phenomenon that produces these effects is called Kerr effect, this is manifested when the refractive index of the material depends on the power of the signal which is being propagated through this material:

$$n(z) = n_L + \Delta n = n_L + n_2 \frac{P(z)}{A_e} \tag{3.9}$$

In the preceding formula $n_L$ is the conventional refractive index, $n_2$ is the non-linear refractive index and $A_e$ is the effective area of the fundamental mode which may be approximated by the core area. It can be observed then that the non-linear effects depend more on the power density per unit area than the absolute power.

- *Self phase modulation* (SPM)

  It consists in a phase modulation of the signal produced by variations of the power of the signal itself. Even if SPM by itself does not modify the width of the signal, this cannot be assured in the presence of dispersion, since when these two interact they might compensate each other or might cause the deterioration of the signal.

- *Cross phase modulation* (XPM)

  It consists in a phase modulation of the signal produced by variations of the power of spectrally adjacent channels. These phase fluctuations may be turned into amplitude fluctuations in the presence of dispersion causing a deterioration of the signal.

- *Four wave mixing* (FWM)

  It causes transfer of energy between the different channels and generates new frequencies.

# Chapter 4

# Maximum likelihood sequence estimation (MLSE)

The maximum likelihood sequence estimation (MLSE) is an optimum sequence detection technique because it minimizes the error probability in making a decision on the transmitted sequence. In this chapter the maximum likelihood principle, metric statistics and the Viterbi algorithm are discussed.

## 4.1 Maximum likelihood

Generally speaking, let us consider a model which gives the probability density function of observable random variable $X$ as a function of a parameter $\theta$. Then, for a specific value $x$ of $X$, the function $L(\theta|x) = P(X=x|\theta)$ is a likelihood function of $\theta$: it gives a measure of how "likely" any particular value of $\theta$ is, knowing that $X$ has the value $x$. So, a likelihood function arises from a conditional probability distribution considered as a function of its second argument, holding the first one fixed.

In a sense, likelihood has an opposite behaviour than probability: if "probability" allows predicting unknown outcomes based on known parameters, then "likelihood" allows determining unknown parameters based on known outcomes.

The extent to which the evidence supports one parameter value against another is equal to the ratio of their likelihoods. That is:

$$\Lambda = \frac{P(X = x \mid a)}{P(X = x \mid b)} \tag{4.1}$$

is the degree to which the observation *x* supports parameter value *a* against *b*. If this ratio is 1, the evidence is indifferent, and if greater or less than 1, the evidence supports *a* against *b* or vice versa.

The basis for the method of maximum likelihood is that the parameter value which maximizes the likelihood function is the value which is most strongly supported by the evidence.

All this can be applied to a transmission system. Let us suppose that we are to receive the signal vector $r = [r_0, r_1, ..., r_{N-1}]$, and considering that $S_t$ represents one of all the possible transmitted sequences $[s_0, s_1, ..., s_{N-1}]$, the optimum decision rule is that the sequence $S_t$ that maximizes the probability

$$p(S_t / r) = \frac{f(r \mid S_t)\, p(S_T)}{f(r)} \tag{4.2}$$

corresponds to the transmitted sequence $S_T$. This can be reduced to a maximum likelihood rule:

$$s(r) = \arg\max_{S_t} f(r \mid S_t) \tag{4.3}$$

where the functions $f(r / S_t)$ are the likelihood functions.

The sequence most likely to have been transmitted is the one associated with the minimum Euclidean distance (between the received signal *r* and the possible transmitted sequence $S_t$):

$$D(r, S_t) = \sum_{k=0}^{N-1} (r_k - s_k)^2 \tag{4.4}$$

This is called metric, and it can be rewritten as:

$$\Lambda(S_t) = \sum_{k=0}^{N-1} \lambda(x_k, x_{k+1}) \tag{4.5}$$

where $x_k$ is the integer representation of the symbol vector $[s_{k-L+1}, s_{k-L+2}, ..., s_{k-1}]$ consisting of ($L$-1) consecutive data symbols.

Equation 4.5 expresses the optimal metric as the summation of partial metrics $\lambda(x_k, x_{k+1})$. The $k$-th of these terms, $\lambda(x_k, x_{k+1})$, depends on the vectors of consecutive trial symbols $[s_{k-L+1}, s_{k-L+2}, ..., s_{k-1}]$ and $[s_{k-L+2}, s_{k-L+3}, ..., s_k]$ respectively.

These considerations suggest a recursive formula for the evaluation of $\Lambda(S_t)$. So the following recursive relation is defined [4]:

$$\Lambda(s_k) = \Lambda(s_{k-1}) + \lambda(x_k, x_{k+1}) \tag{4.6}$$

with $s_i = [s_0, s_1, ..., s_i]$ $(s_{N-1} = S_t)$ and $\Lambda(s_0) = 0$, then, after $N$ iterations:

$$\Lambda(S_t) = \Lambda(s_{N-1}) \tag{4.7}$$

A geometrical representation of the problem of searching over the optimal metric can be given as follows. A trellis diagram with $N_s$ states is drawn as in Figure 4.1. In the $k$-th interval each trellis state represents one of the $N_s$ possible values that $x_k$ can take, and it is connected via $M$ branches to the next state $x_{k+1}$ (where $M$ is the number of M-ary symbols). The branch connecting the states $x_k$ and $x_{k+1}$ is labeled by the trial symbol $s_k$ and by the branch metric $\lambda(x_k, x_{k+1})$. In this way each trial sequence $S_t$ has a one to one correspondence with a sequence of states in the trellis diagram. Looking for the optimal sequence decision is equivalent to searching for the path with minimum accumulated metric in the trellis. Such search would require an exhaustive analysis and comparison between all the possible trial sequences (trellis paths); in fact, for a sequence of $N$ symbols, about $M^N$ comparisons would have to be performed to select the most likely sequence, so the number of computations grows exponentially with respect to *N*. This technique would be unacceptable due to its excessive complexity; however, this can be carried out recursively employing the *Viterbi algorithm*, where the number of computations necessary to select the most likely sequence grows only linearly. The Viterbi algorithm will be discussed later in section 4.3.

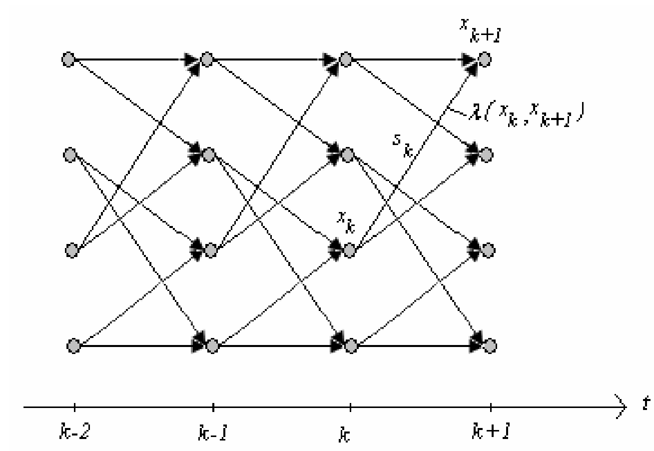


Figure 4.1. 4-state trellis diagram (M=2 is assumed)

## 4.2 Branch metric statistics

At it has been said before, the MLSE processor is implemented using the Viterbi algorithm. At each processor iteration, the following metric should be evaluated for each trellis branch:

$$M^{(n)} = -\sum_{k=1}^{K} \ln\left\{ f_{y_{n,k}}(y) \right\} \tag{4.8}$$

where *n* is an index running from 1 to the total number of branches in the trellis, *k* is an index running from 1 to the total number *K* of samples per bit, $y_{n,k}$ is the random variable associated to the noisy signal, being the transmitted signal the one associated to the *n*-th branch of the *k*-th sample, $f_{y_{n,k}}(y)$is the probability density function (pdf) of $y_{n,k}$ and $y$ is the actual noisy signal sample taken on the photo-detected electrical signal $y(t)$.

It is seen that the metric expression takes account of the exact pdf's of the signal samples. However, such pdf's are not analytically available in optical systems using post-detection filtering, and semi-analytical techniques based on Karhunen-Loève expansion [5] are needed to correctly evaluate them.

In order to reduce the computational complexity, in practice some other statistic models that approximate the signal statistic can be used to calculate the branch metrics.

Some of the models that approximate the signal statistic in an optical system are based on the assumption that the distribution of the received signal samples is Gaussian. In the following, two different metrics based on this assumption are described.

### 4.2.1 Gaussian metric

It is possible to simplify the metric evaluation procedures by assuming that the received signal samples are uncorrelated and follow a Gaussian distribution.

The Gaussian metric assumes an additive non-stationary Gaussian noise distribution. Its expression is the following:

$$M_{GAUSS}^{(n)} = -\sum_{k} \left\{ \frac{(y_k - \mu_{n,k})^2}{\sigma_{n,k}^{\ 2}} + \ln(\sigma_{n,k}^{\ 2}) \right\} \tag{4.9}$$

where $y_k$ is the $k$-th noisy received sample, and $\mu_{n,k}$ and $\sigma_{n,k}^{\ 2}$ are the mean value and the variance of the $k$-th signal sample for the $n$-th trellis branch respectively.

The Gaussian metric correctly takes the noise variance non-stationarity into account, but as a consequence, a matrix $\sigma_{n,k}^{\ 2}$ must be estimated and its values must be recalled at run-time to evaluate each signal sample contribution to the metric, which makes it very computationally intensive.

### 4.2.2 Square-root metric

The square-root metric is a simplified metric in which it is assumed that the square-root of the received signal follows a Gaussian distribution and that the variance of the square-root of the received signal samples is stationary [6].

Under these assumptions the square-root branch metric has the following expression:

$$M_{SQRT}^{(n)} = -\sum_{k}\left(\sqrt{y_k} - \mu'_{n,k}\right)^2 \tag{4.10}$$

where $y_k$ is the $k$-th noisy received sample, and $\mu'_{n,k}$ is the mean value of the $k$-th signal sample for the $n$-th trellis branch.

This metric has the advantage that only the average value of the signal has to be calculated during the channel estimation procedure, and its expression can be written in a simple closed form.

## 4.3 Viterbi algorithm

The application of the Viterbi algorithm consists on finding, among the paths traversing the trellis from left to right (from time $k = 0$ until time $k = N$), the one with minimum metric. The metric associated with a path is the sum of the labels of the branches forming the path.

Formally, if $x_k$ denotes the state at time $k$, taking values $\{X_i\}_{i=1}^{Ns}$, and $\lambda(x_k, x_{k+1})$ denotes the metric associated with the branch emanating from node $x_k$ and joining node $x_{k+1}$, the algorithm tries to minimize the function:

$$\Lambda(x_0, x_1, ..., x_{N-1}) = \sum_{k=0}^{N-1} \lambda(x_k, x_{k+1}) \tag{4.11}$$

over the possible choices of the state sequences $(x_0, \ldots, x_{N-1})$ compatible with the trellis structure.

The problem above could be solved by a brute-force approach, consisting of evaluating all the possible values of the function $\Lambda$ and choosing the smallest. However, this would be too complex to develop due to the number of computations required and the storage needed, as they grow exponentially with the length $N$ of the sequence.

The Viterbi algorithm solves the minimization problem without suffering from exponential complexity, actually its computational complexity grows only linearly with $N$.

The Viterbi algorithm achieves this by using a three key steps procedure: Add, Compare and Select (ACS). Consider Figure 4.2 in which the trellis states at time $k$ and $k+1$ are shown. The branches which link the states are labeled by the corresponding branch metrics, while the states are labeled by the *accumulated state metrics* which will be defined later. The add, compare and select procedure consists on the following:

- For each state $x_{k+1}$, examine the branches stemming from states $x_k$ and leading to it. For these branches *add* the metric accumulated at the state $x_k$ to the metric of the branch itself.
- *Compare* the results of these sums.
- *Select* the branch associated with the minimum value and discard all the other branches (if the quantities being compared are equal, either one of them can be chosen randomly). This minimum value is associated with the state $x_{k+1}$ and forms its state accumulated metric (this value is stored only for the next ACS step and then discarded).

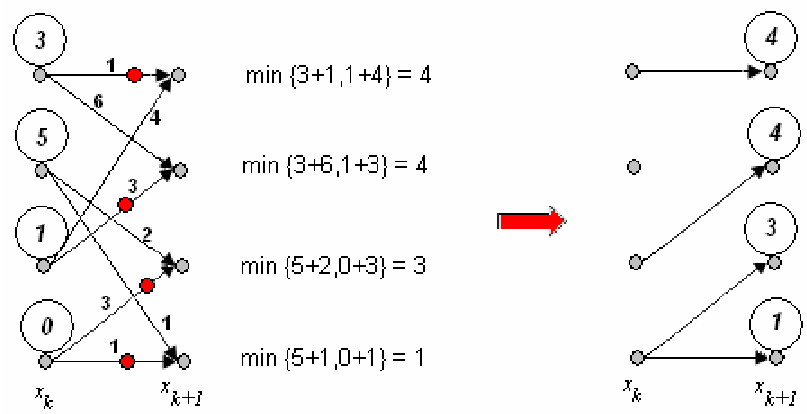


Figure 4.2. ACS step of Viterbi algorithm

The Viterbi algorithm consists of repeating the ACS from the first state of the trellis to the last state. After each ACS step for each state one value of accumulated metric and one path are retained. Thus, at any time $k$, for each $x_k$ there is just a single survivor path left traversing the trellis from its first state to $x_k$ and one value of accumulated metric. This survivor path is the minimum-metric path to the corresponding state. After $N$ ACS steps, at the termination of the trellis, a single $N$-branch path and an accumulated metric are obtained, which are the minimum metric path and the minimum metric value respectively [7].

Figure 4.3 shows an example of the determination of the minimum metric path through a 4 states trellis using the Viterbi algorithm with $N$=6.

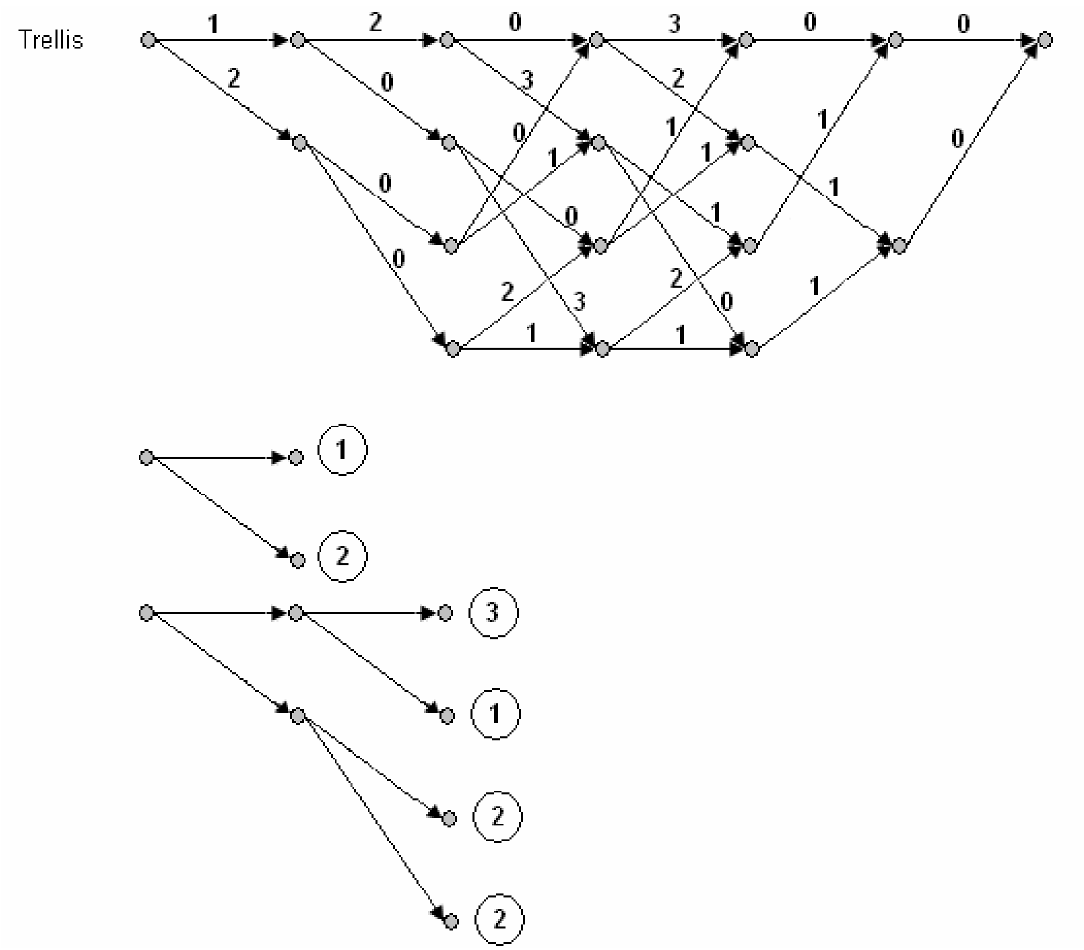
Trellis

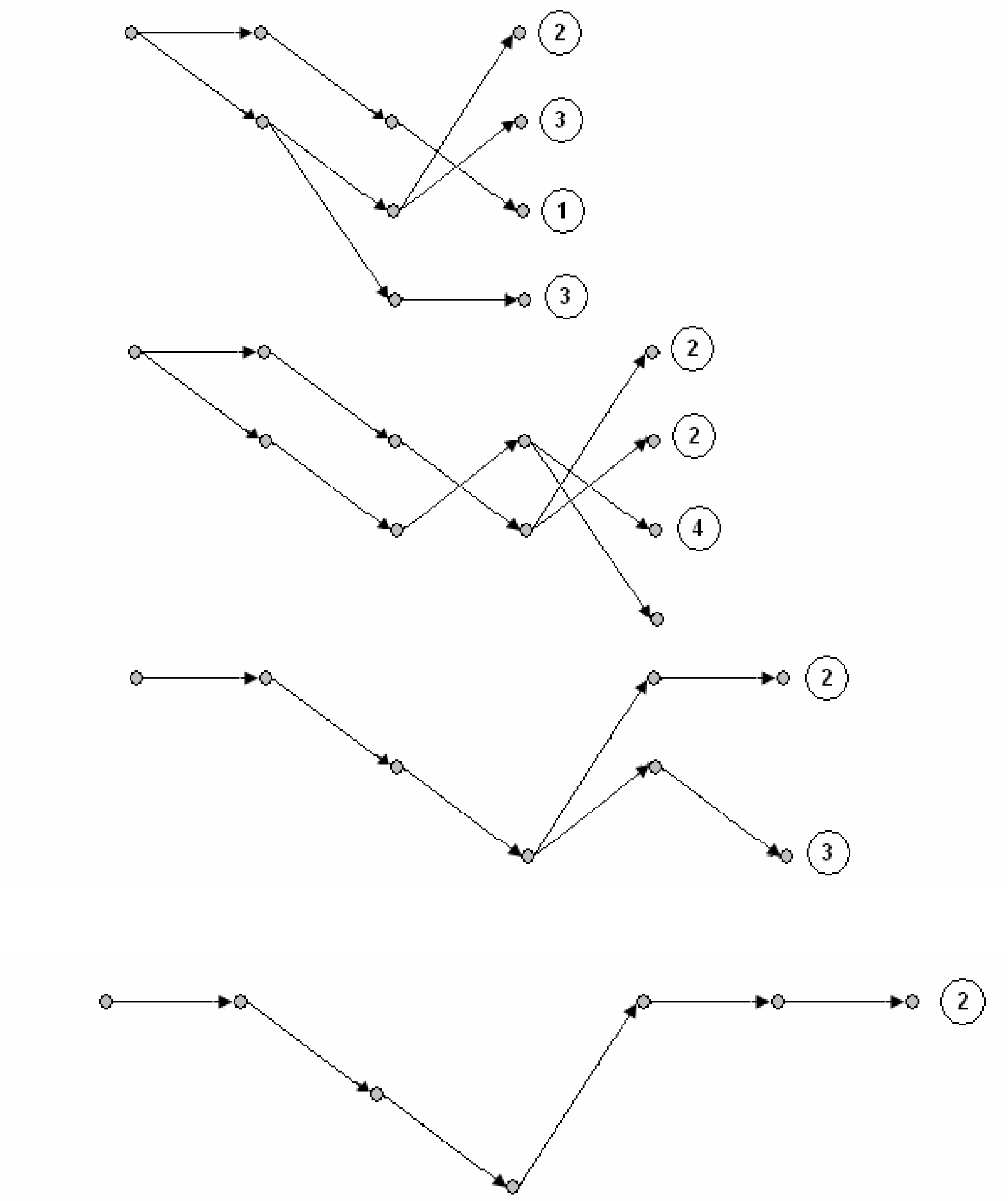


Figure 4.3. Determination of the minimum metric path using the Viterbi algorithm

# Chapter 5

# Performance of the MLSE equalization in an optical communication system using a purely dispersive fiber

In this chapter the results of a study done on the advantages of the use of the MLSE equalization in an optical communications system using a purely dispersive fiber are shown.

A purely dispersive fiber is used in order to measure how the use of MLSE receivers strengthens the robustness to chromatic dispersion of the IMDD modulation format and other alternative modulation formats; as Duobinary (DB) and 2- and 4-level Differential Phase Shift Keying (DPSK and DQPSK). The advantages of the use of the Gaussian and Square-root metric by the MLSE processor are analyzed as well.

First, the joint effect of MLSE and filter optimization is studied, and then several configurations to upgrade the systems as the insertion of an optical filter at the transmitter, the application of the MLSE equalization in each branch of the receiver of the DPSK and DQPSK systems and the use of a 2bit/symbol parallel MLSE processor for the DQPSK system are studied.

The simulations of the optical system were done using the software Optsim, and the MLSE processor was implemented using Matlab.

# 5.1 Study of the simultaneous use of MLSE equalization and optimal filters

Since the optimization of the receiver's optical and electrical filters can improve the performance as well as the MLSE equalization, the simultaneous use of both techniques yields even better results.

In this section, the advantages of the use of MLSE on systems based on typical Rx filters are shown; then, the Rx filters are optimized showing the advantages of simultaneous use of MLSE and optimal filters for IMDD, DB, DPSK and DQPSK modulation formats.

## 5.1.1 System characteristics

The characteristics of the system set-up and simulation procedures are the following:

- The bit-rate is $R_b$ 10 Gbit/s.
- The Pseudo-Random Bit Sequence is PSRB = $2^{16} - 1$ = 65535 bits.
- Each bit is simulated using 20 samples.
- For DB, DPSK and DQPSK modulations the PRBS is properly precoded.
- A single span of a purely dispersive fiber is used with:
  D = 16 ps/nm/Km
- The ASE noise is added at the end of the fiber to obtain the desired Optical Signal to Noise Ratio (OSNR) which is measured over a noise bandwidth equal to the bit-rate.
- The receiver is assumed noiseless.

- The receiver is composed of a second order Supergaussian optical filter with bandwidth $B_o$, followed by an ideal photodetector and a fifth order Bessel electrical filter with bandwidth $B_e$. For the DPSK and DQPSK systems between the optical filter and the photodetector there is a 1-bit-delay Asymmetric Mach-Zehnder Interferometer.
- At the receiver's end, 4 samples per bit are taken.
- The receiver is followed by an MLSE processor, which consists of an A/D converter whose samples are sent to a parallel bank of 64 branch metric computation stages followed by a 32-states Viterbi processor.
- No optimization of the sampling instant is done at the receiver.
- For IMDD and DB, 2 samples per bit are used for the branch metric evaluation. For DPSK and DQPSK, 4 samples per bit are used instead, being more sensitive than IMDD and DB to the sampling instant within the bit slot.
- The system performance is measured according to the OSNR necessary to reach a BER value equal to $10^{-3}$, which ensures the operation below the FEC threshold.
- Simulations: Using an optical simulator, we first obtained the received filtered electrical signal for various values of OSNR and distance (L). For each value of OSNR and L, the RX signal was processed by the MLSE circuit, searching for the OSNR yielding the target performance of bit error rate (BER) equal to $10^{-3}$.

### 5.1.2 IMDD-NRZ modulation

The system set-up is shown in Figure 5.1.

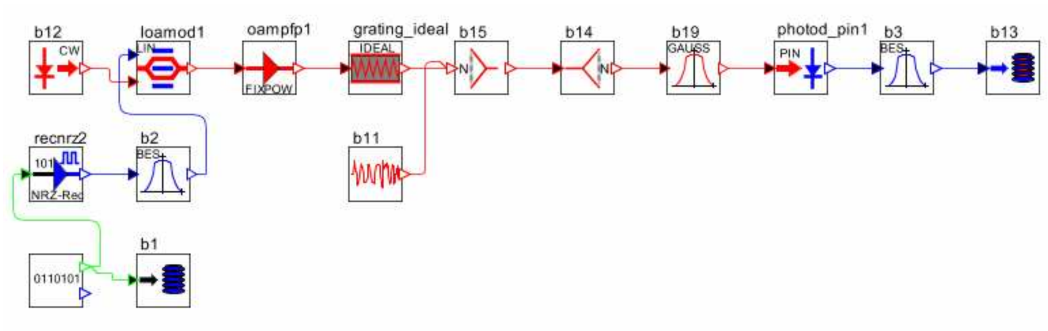


Figure 5.1. IMDD system set-up

First, the bandwidths of the optical and electrical filters were set to 50 GHz and 7.5 GHz respectively, which are the typical non optimized bandwidths. The performance of this system is shown in Figure 5.2. In this figure a comparison is done between the system in which the sqrt metric is used and the system in which the Gaussian metric is used; and a reference curve obtained by evaluating the system performance without MLSE through direct error counting is shown as well.

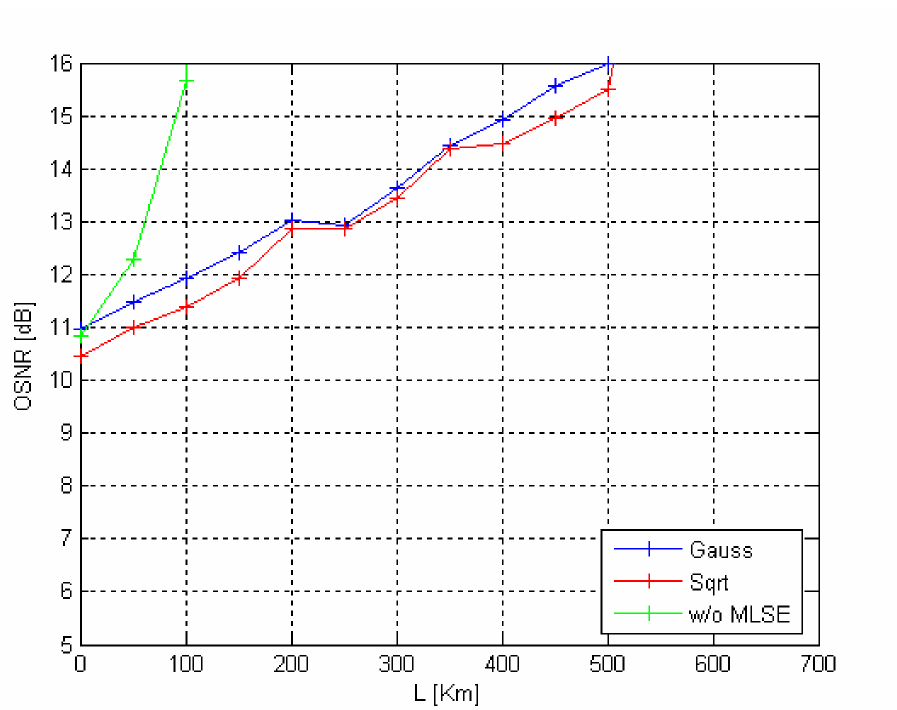


Figure 5.2. OSNR vs L for the IMDD system with typical bandwidths

As it is seen, the performance of the system in which the equalization is not used is visibly worse than the performance of the other systems, which shows how the use of MLSE equalization strengthens the robustness to chromatic dispersion allowing the system to go further without the use of optical compensation. It is also observed that the system in which the sqrt metric is used, has a better performance than the system in which the Gaussian metric is used.

At this point, the optimization of the reception filters was done. To do this, a point in the curve is conveniently chosen, setting the values for distance and OSNR, and then the electric and optic bands are swept in an appropriate grid, obtaining a BER value for each couple of bands. Then, the couple of bands that provides the minimum BER value is considered the optimal. This procedure is done using the metric that shows better performance.

So, following the procedure described previously, the optimization was done at a distance of 185 Km, and using the sqrt metric for the branch metric evaluation in the MLSE processor.

As a result of the optimization, Figure 5.3 was obtained. In this figure, the highest point corresponds to the lowest BER value, so the optimal bands are defined by it. As it can be seen, the optimum band of the optical filter is 9 GHz and the optimum band of the electric filter is 24 GHz. As expected, the optical band is around the value of the bit-rate, and the electric band is wider.

The performance of the system in which the optimized filters are used is shown in Figure 5.4.

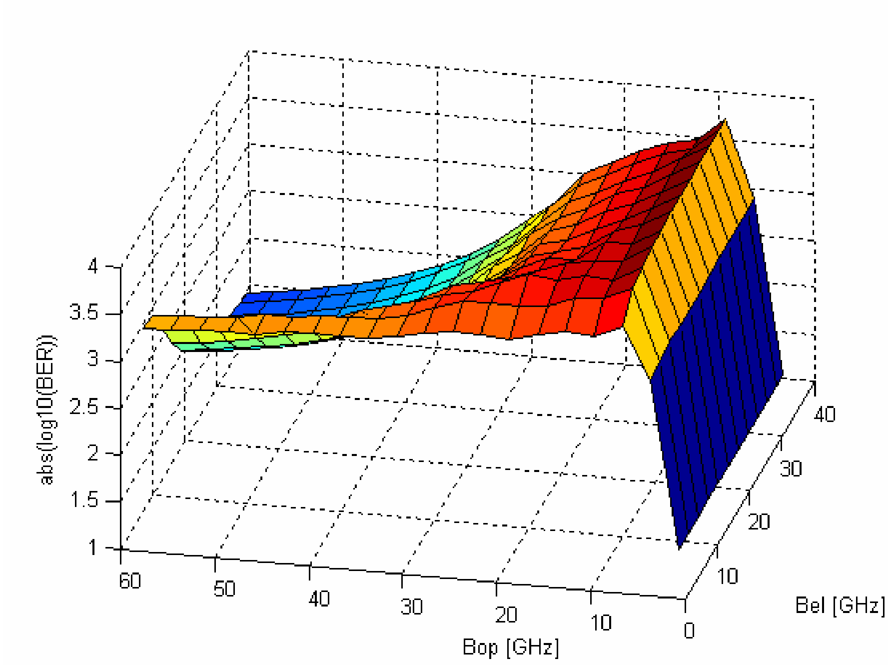


Figure 5.3. Optimization of the filters for the IMDD system

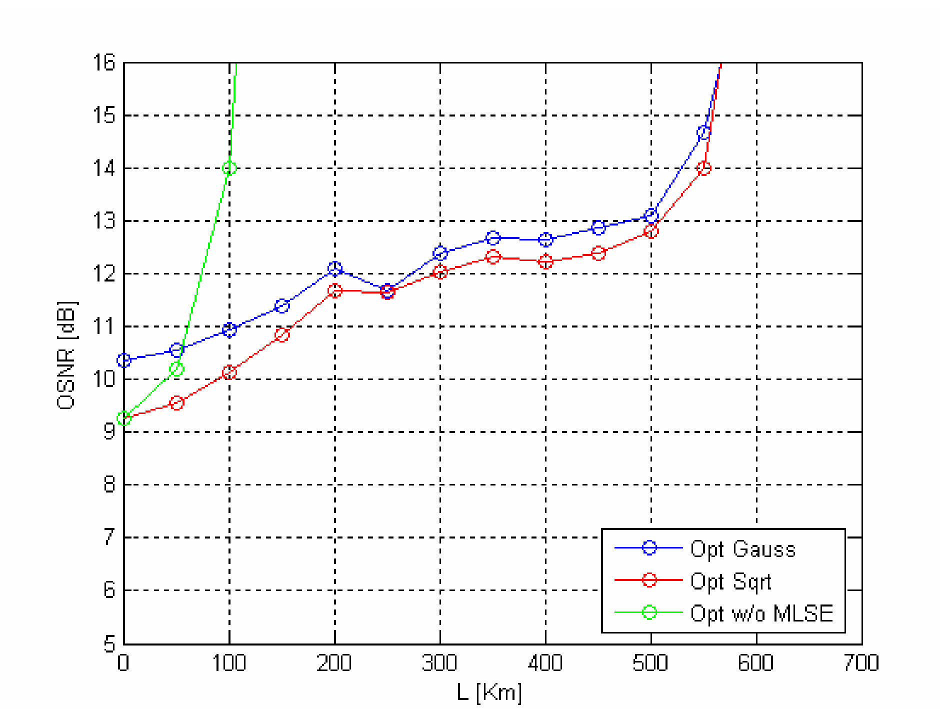


Figure 5.4. OSNR vs L for the IMDD system with optimum filters

In order to make a comparison with the results obtained previously, Figure 5.5 shows all the results obtained until now.

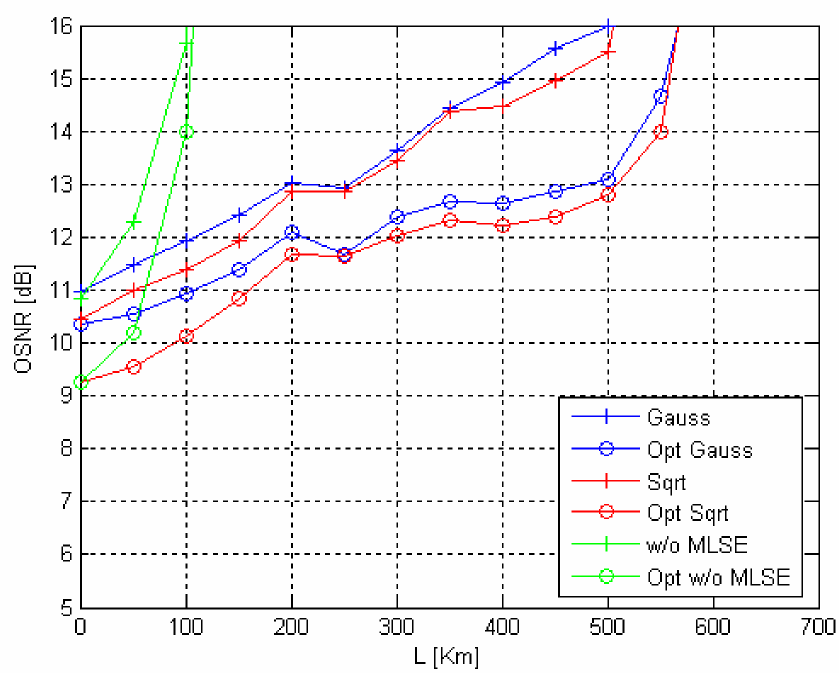


Figure 5.5. Performance of the IMDD system

As it can be seen, the system that shows better performance is the one in which the sqrt metric and the optimum filters are used.

Figure 5.5 shows that, without the filter optimization, the use of the MLSE processor with sqrt metric allows to extend from 60 Km to 250 Km the distance at which the OSNR penalty is 2 dB with respect to the back to back performance without MLSE. With filter optimization, the use of the MLSE processor with sqrt metric allows to reach 300 Km for an OSNR equal to 12 dB.

## 5.1.3 Duobinary modulation

The system set-up is shown in Figure 5.6.

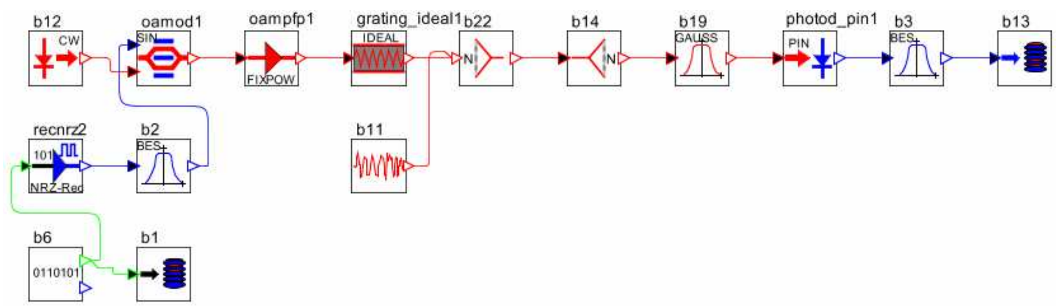


Figure 5.6. Duobinary system set-up

First, the bandwidths of the optical and electrical filters were set to 50 GHz and 7.5 GHz respectively. Then, the optimization of the bandwidths was done at a distance of 610 Km obtaining an optimum optical bandwidth equal to 8 GHz and an optimum electrical bandwidth equal to 29 GHz.

The performance of these systems is shown in Figure 5.7. In this figure, a comparison is done between the system in which the sqrt metric is used and the system in which the Gaussian metric is used; and a reference curve obtained by evaluating the system performance without MLSE through direct error counting is shown as well.

It can be observed that, the system that shows better performance is the one using the optimum filters and the MLSE processor with the sqrt metric; even though the performance experiences a slight back to back penalty when using MLSE.

Figure 5.7 shows that the use of MLSE is very effective for the system with Duobinary modulation, keeping its performance almost constant (within 2 dB OSNR penalty) up to 600 Km. For Duobinary, the advantage of using the sqrt metric is still present, but it is lower than for IMDD. The filter optimization is really effective as it allows reaching 650 Km for an OSNR equals to 12 dB.

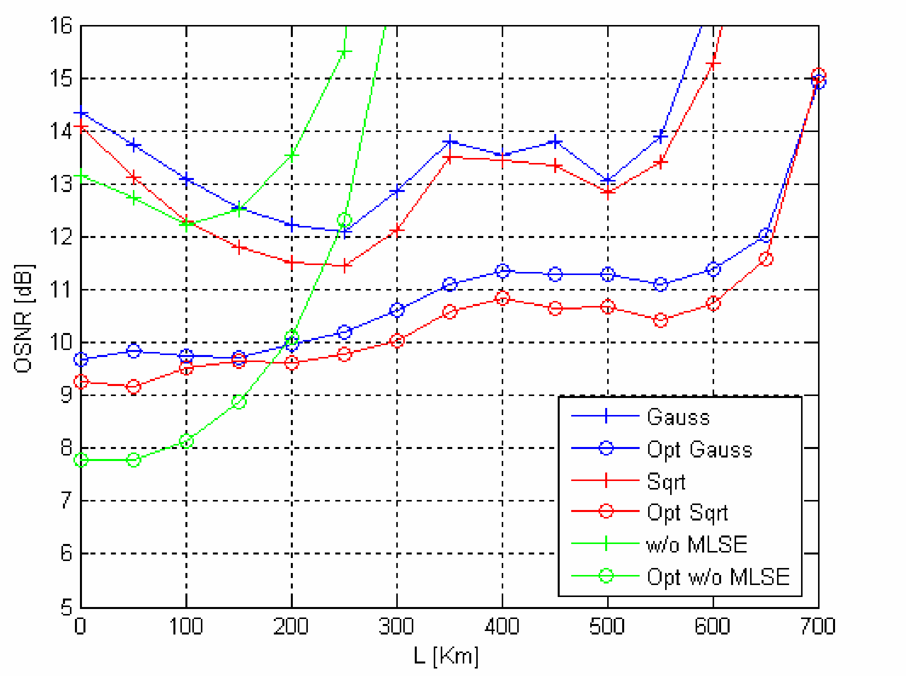


Figure 5.7. Performance of Duobinary system

## 5.1.4 DPSK modulation

The system set-up is shown in Figure 5.8.

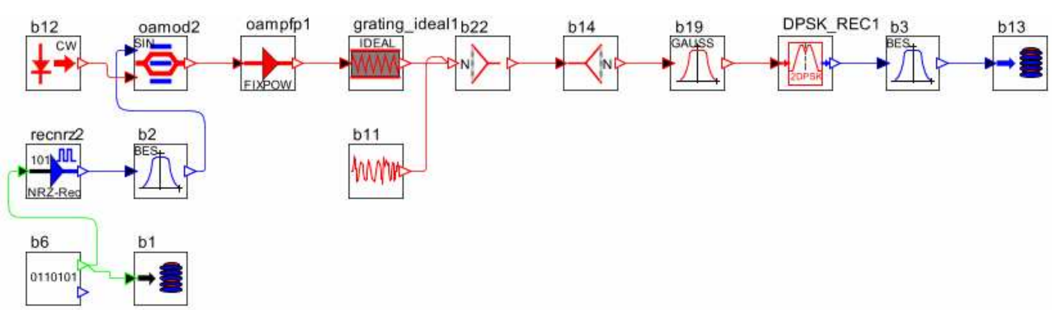


Figure 5.8. DPSK system set-up

For the DPSK modulation, because of the nature of the decision signal which is symmetric around the zero level and thus takes also negative values, the sqrt metric cannot be applied, so only the Gaussian statistic was considered.

First, the bandwidths of the optical and electrical filters were set to 50 GHz and 7.5 GHz respectively. Then, the optimization of the bandwidths was done at a distance of 200 Km obtaining an optimum optical bandwidth equal to 10 GHz and an optimum electrical bandwidth equal to 33 GHz.

The performance of these systems is shown in Figure 5.9. A reference curve obtained by evaluating the system performance without MLSE through direct error counting is shown as well.

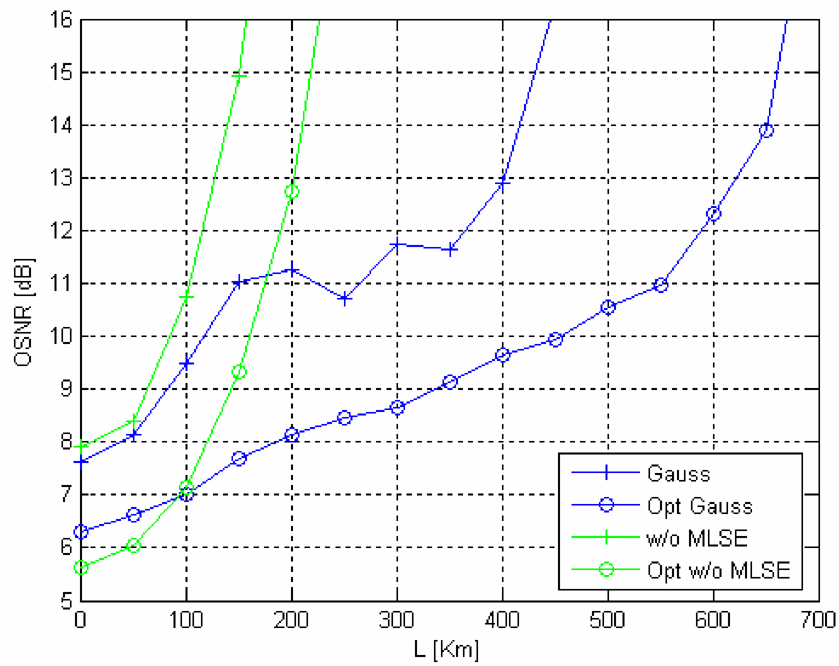


Figure 5.9. Performance of DPSK system

Figure 5.9 shows that the advantages of MLSE for DPSK are limited in absence of filter optimization, while using the optimal filters together with the MLSE, the system reaches almost 600 km for an OSNR equal to 12 dB. It is also seen that, the system experiences a slight back to back penalty when using MLSE.

## 5.1.5 DQPSK modulation

The system set-up is shown in Figure 5.10.

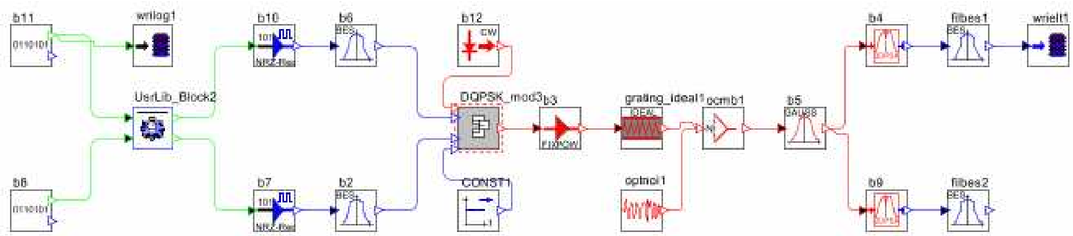


Figure 5.10. DQPSK system set-up

For the DQPSK modulation, because of the nature of the decision signal which is symmetric around the zero level and thus takes also negative values, the sqrt metric cannot be applied, so it only the Gaussian statistic was considered.

First, the bandwidths of the optical and electrical filters were set to 50 GHz and 7.5 GHz respectively. Then, the optimization of the bandwidths was done at a distance of 300 Km obtaining an optimum optical bandwidth equal to 9 GHz and an optimum electrical bandwidth equal to 19 GHz.

The performance of these systems is shown in Figure 5.11. A reference curve obtained by evaluating the system performance without MLSE through direct error counting is shown as well.

Figure 5.11 shows that the use of MLSE for DQPSK even in the case of filter optimization, gives limited advantages. The system using DQPSK modulation with MLSE and optimal filters can reach 400 Km for an OSNR equal to 12 dB, extending only by 100 Km the performance of the standard receiver without filter optimization.

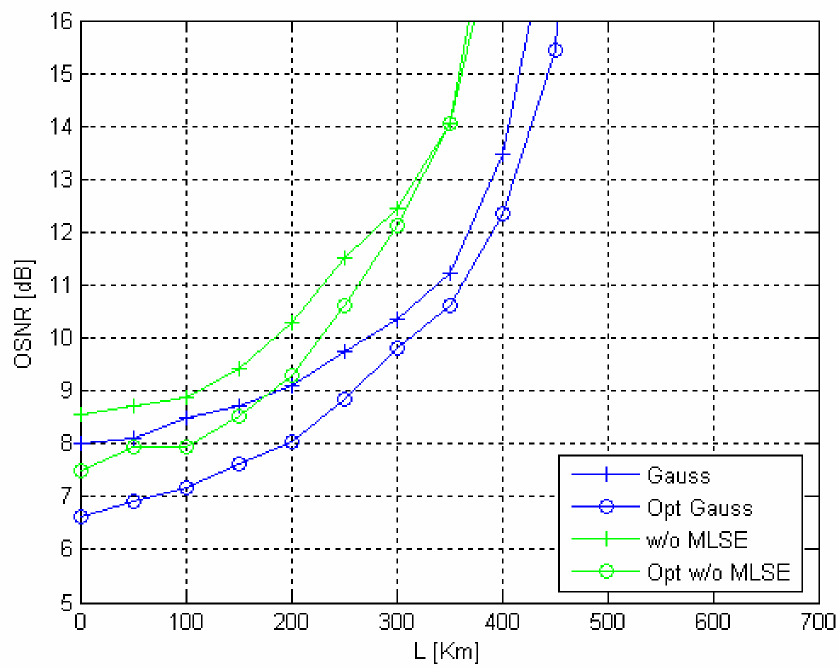


Figure 5.11. Performance of DQPSK system

## 5.2 Upgrading of the systems

In this section the results of some studies that were done in order to further improve the performance of the systems that were presented in section 5.1 are shown.

### 5.2.1 IMDD-NRZ modulation

- **Insertion of an optical filter in the transmitter**

An optical filter was inserted in the transmitter of the system presented in section 5.1.2 in order to check whether sending the signal with a narrower bandwidth yields better result, as the action of dispersion is reduced.

The system set-up is shown in Figure 5.12. In this system, the value of the optical filter in the receiver was set to 50 GHz and the optimization of the optical filter in the transmitter and the electrical filter in the receiver was done.

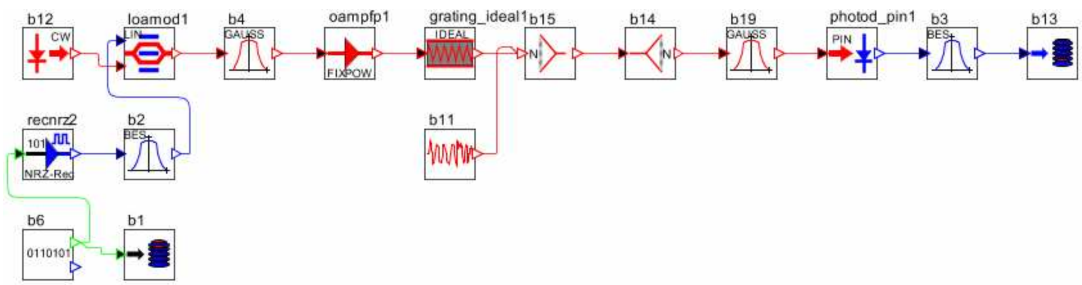


Figure 5.12. IMDD system with optical filter in the transmitter

The optimization was done at a distance of 185 Km, obtaining 24 GHz as the optimum bandwidth of the optical filter and 9 GHz as the optimum bandwidth of the electric filter.  The result of the optimization procedure is shown in Figure 5.13.

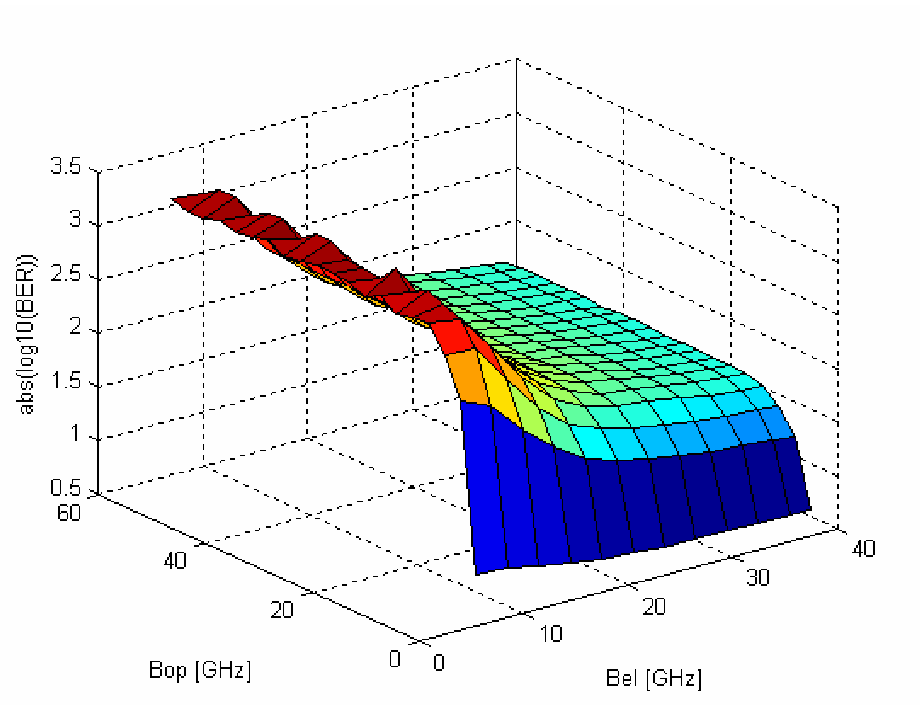


Figure 5.13. Filter optimization for the IMDD system with optical filter in the transmitter

The performance of the system with optimum filters and sqrt metric is shown in Figure 5.14.

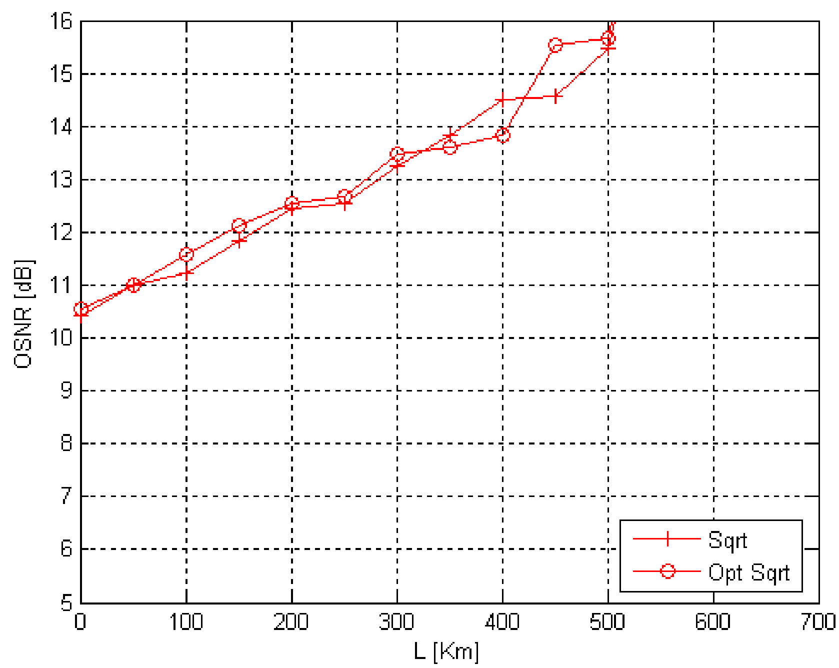


Figure 5.14. Performance of IMDD system with optical filter in the transmitter

As it is seen, the system that uses the bandwidths resulting from the optimization procedure does not show a better performance than the system using the standard bandwidths. Therefore, the better way to set up the system is to put the optical and electric filters in the receiver, since having a narrow optic filter at the front of the receiver cuts out the noise introduced by the channel.

Given the results, the insertion of the optical filter in the transmitter was not studied for other modulation formats.

## 5.2.2 Duobinary modulation

- **Use of 4 samples per bit for the branch metric evaluation**

The number of samples per bit used for the branch metric evaluation was increased from 2 to 4 in order to understand if a better performance would be achieved, since by doing so, the sensitivity to the sample instant within the bit slot would be reduced.

The optimum filters ($B_o$ = 8 GHz and $B_e$ = 29 GHz) were used, and the MLSE processor used the sqrt metric. The result is shown in Figure 5.15.

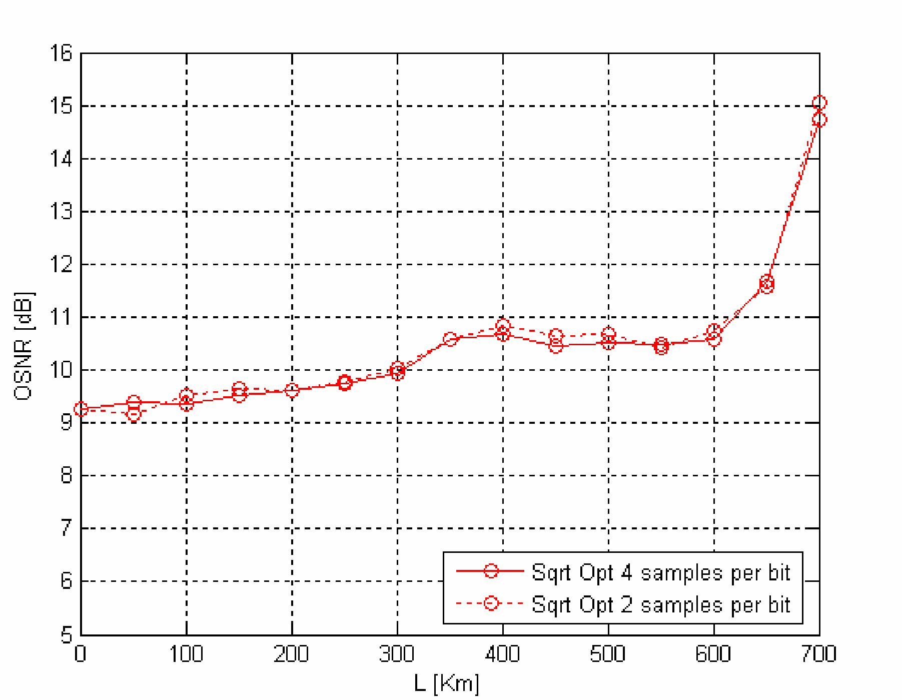


Figure 5.15. Performance of DB system with 4 samples per bit for the branch metric evaluation

It can be observed that the performance of the system that uses 4 samples per bit for the branch metric evaluation is almost the same as the performance of the system using 2 samples per bit. Therefore, the Duobinary modulation is not sensitive to the sampling instant within the bit slot and 2 samples per bit are enough in order to get the best performance.

## 5.2.3 DPSK modulation

- **Use of 8 samples per bit for the branch metric evaluation**

The number of samples per bit used for the branch metric evaluation was increased from 4 to 8 in order to understand if a better performance would be achieved, since by doing so, the sensitivity to the sample instant within the bit slot would be reduced.

The optimum filters ($B_o$ = 10 GHz and $B_e$ = 33 GHz) were used and the MLSE processor used the Gaussian metric. The result is shown in Figure 5.16.

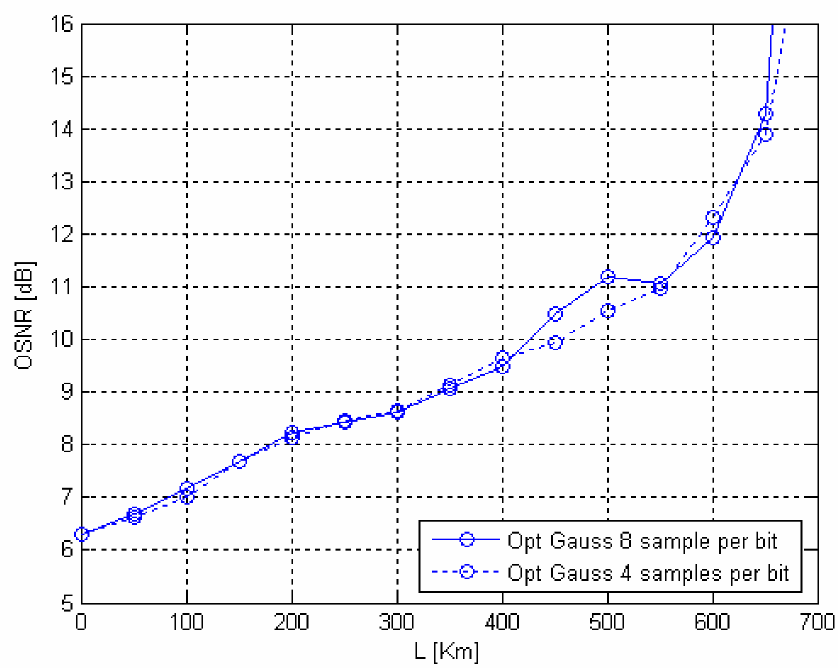


Figure 5.16. Performance of DPSK system with 8 samples per bit for the branch metric evaluation

It can be observed that the performance of the system that uses 8 samples per bit for the branch metric evaluation is almost the same as the performance of the system using 4 samples per bit. Therefore, for the DPSK modulation 4 samples per bit are enough in order to get the best performance.

- **Insertion of the square-root device in each branch of the receiver and use of the sqrt metric**

As it has been seen before, the use of the sqrt metric produces better results than the use of the Gaussian metric for other modulation formats that accept this kind of metric. In order to understand if the sqrt metric could also improve the performance of the DPSK system, a square-root device was inserted in each branch of the DPSK receiver after the electrical filters, and the sqrt metric was used at the MLSE processor. In this system the optimum filters ($B_o$ = 10 GHz and $B_e$ = 33 GHz) are used.

The system is shown in Figure 5.17.

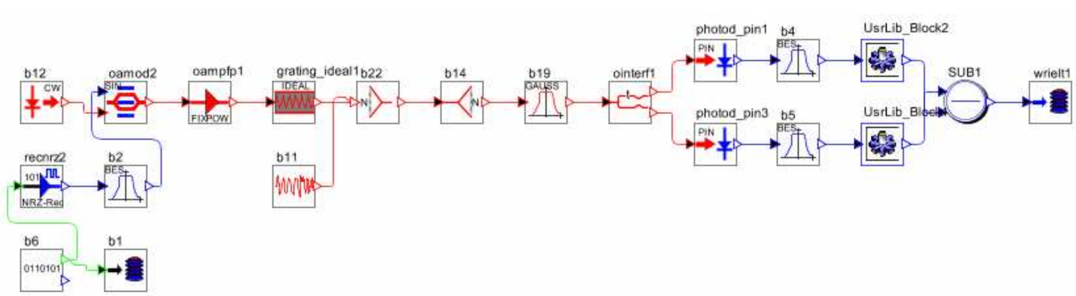


Figure 5.17. DPSK system with square root device in each branch

The result is shown in Figure 5.18. It may be observed that the performance of the system using the sqrt metric is almost the same as the system using the Gaussian metric. Thus, for DPSK, contrary to what happens for the IMDD and Duobinary modulations, the insertion of the square-root device and the use of sqrt metric does not improve its performance.

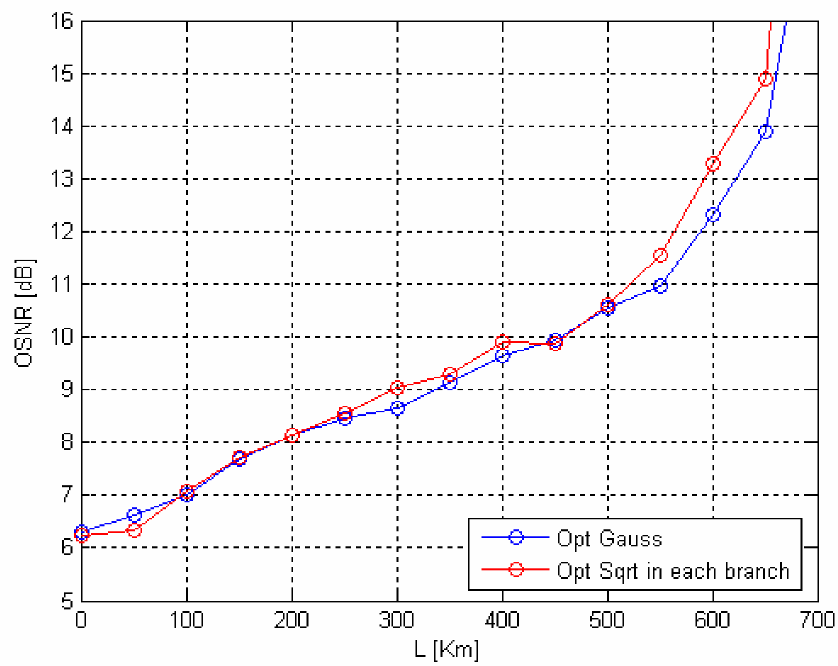


Figure 5.18. Performance of DPSK system with sqrt metric

- **MLSE processor in each branch**

Rather than inserting the MLSE processor right after the standard balanced receiver, the signal samples $y_k^{low}$ and $y_k^{up}$ at the output of the lower and upper photodetector were processed separately.

The new metric used was the addition of the metrics of the two branches. Hence, the metric becomes:

$$M_{DPSK}^{(n)} = -\sum_{k=1}^{4} \ln\left\{f_{up}^{(n)}\left(y_k^{up}\right)\right\} - \sum_{k=1}^{4} \ln\left\{f_{low}^{(n)}\left(y_k^{low}\right)\right\} \tag{5.1}$$

where $f_{low,up}{}^{(n)}(y_k)$ is the probability density function of the signal samples on the *n*-th trellis branch. For simplicity, it is supposed that the probability density function follows a Gaussian distribution.

Figure 5.19 shows the system set-up.

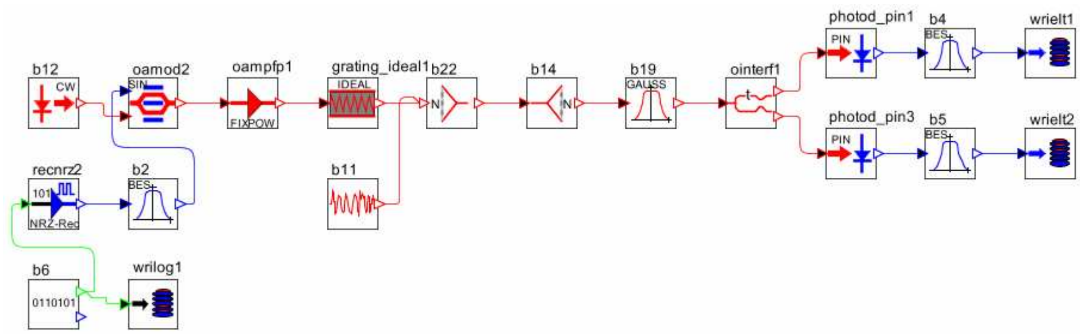


Figure 5.19. DPSK system with MLSE processor in each branch

First, the bandwidths of the optical and electrical filters were set to 50 GHz and 7.5 GHz respectively. Then, the optimization of the bandwidths was done at a distance of 300 Km obtaining an optimum optical bandwidth equal to 14 GHz and an optimum electrical bandwidth equal to 22 GHz.

The results are shown in Figure 5.20.

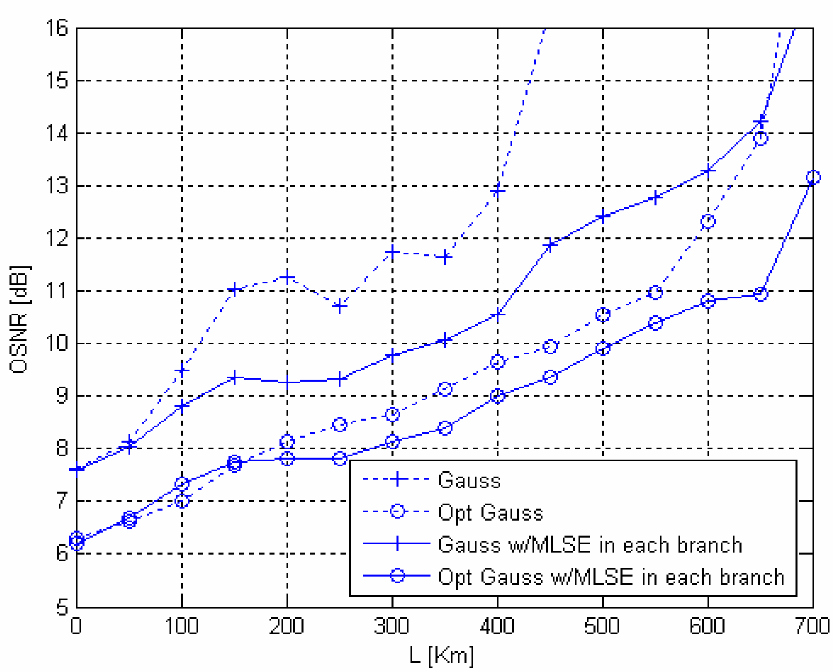


Figure 5.20. Performance of DPSK system with MLSE in each branch

Figure 5.20 shows that, by using MLSE in each branch, the DPSK system can reach 460 Km without filter optimization and 670 Km with filter optimization for an OSNR equal to 12 dB. So it is concluded that this is the most effective way (among the studied) to implement a system that uses DPSK modulation.

## 5.2.4 DQPSK modulation

- **MLSE processor in each branch**

Rather than inserting the MLSE processor right after the standard balanced receiver, the output of the lower and upper photodetector were processed separately, using the metric shown in equation 5.1. Figure 5.21 shows the system set-up.

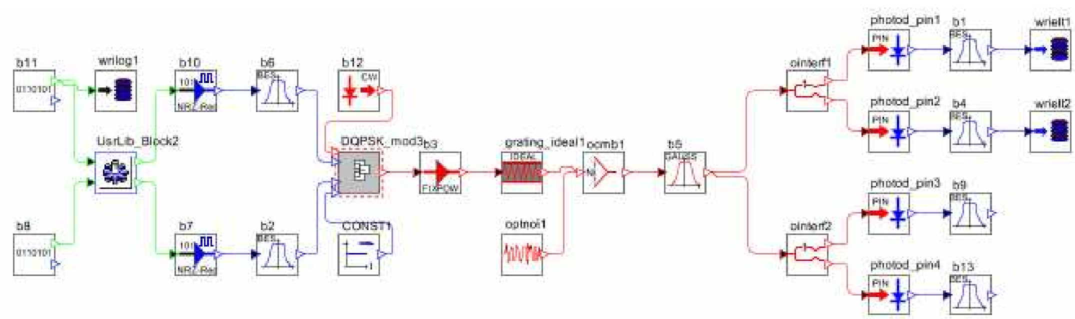


Figure 5.21. DQPSK system with MLSE processor in each branch

First, the bandwidths of the optical and electrical filters were set to 50 GHz and 7.5 GHz respectively. Then, the optimization of the bandwidths was done at a distance of 300 Km obtaining an optimum optical bandwidth equal to 15 GHz and an optimum electrical bandwidth equal to 19 GHz. The results are shown in Figure 5.22.

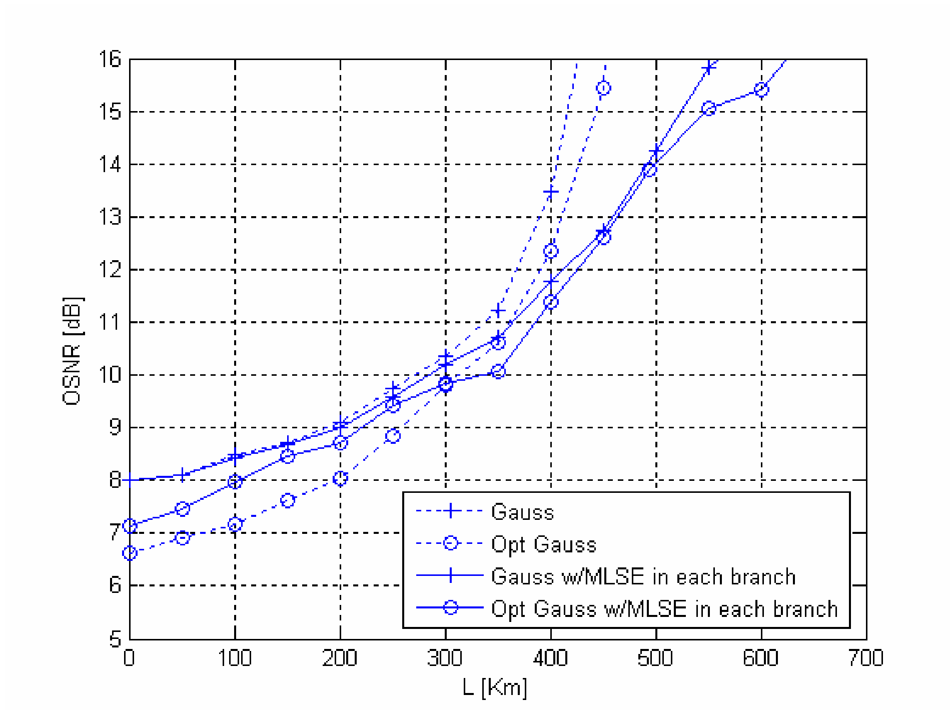


Figure 5.22. Performance of DPSK system with MLSE in each branch

It is seen that, for DQPSK, the use of MLSE equalization in each branch of the receiver, does not give much better results than the use of the MLSE processor right after the standard balanced receiver.

- **Use of a 2 bit/symbol 4-states parallel MLSE processor**

Two balanced receivers were used for detecting the in-phase $y_k^I$ and quadrature $y_k^Q$ signal components, and a MLSE processor that makes joint decisions on the signal samples $y_k^I$ and $y_k^Q$ was inserted.

The metric used assumes the following expression:

$$M_{DQPSK}^{(n)} = -\sum_{k=1}^{4} \ln\left\{ f^{(n)}\left(y_k^I, y_k^Q\right) \right\} \tag{5.2}$$

where $f^{(n)}\left(y_k^I, y_k^Q\right)$ represents the joint probability of receiving the two samples $y_k^I$ and $y_k^Q$

for the *n*-th trellis branch. A Gaussian distribution is assumed for the probability density function of the electrical signal samples.

The joint MLSE processor uses a 4 state trellis and operates over symbols composed by 2 bits, which corresponds to a binary MLSE processor with $4^2$=32 states.

Figure 5.23 shows the system set-up.

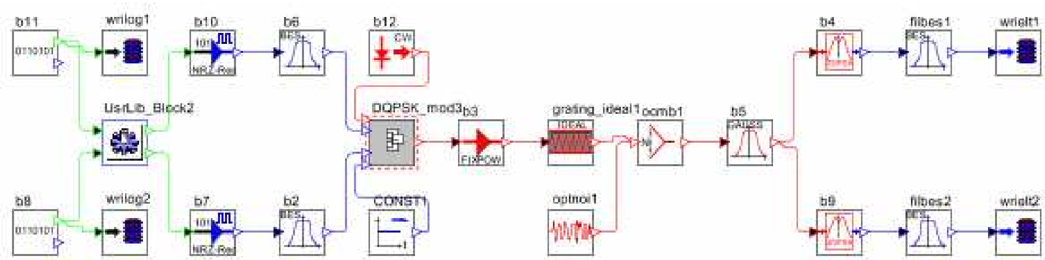

Figure 5.23. DQPSK system with 2 bit/symbol parallel MLSE processor

First, the bandwidths of the optic and electrical filters were set to 50 GHz and 7.5 GHz respectively. Then, the optimization of the bandwidths was done at a distance of 600 Km obtaining an optimum optical bandwidth equal to 6 GHz and an optimum electrical bandwidth equal to 14 GHz. The results are shown in Figure 5.24.

These results confirm that a 2 bit/symbol 4-states parallel MLSE processor is very effective, as its use combined with filter optimization allows reaching 700 Km experiencing only less than 2 dB penalty with respect to the back to back performance (which requires an OSNR equal to 6.6 dB).

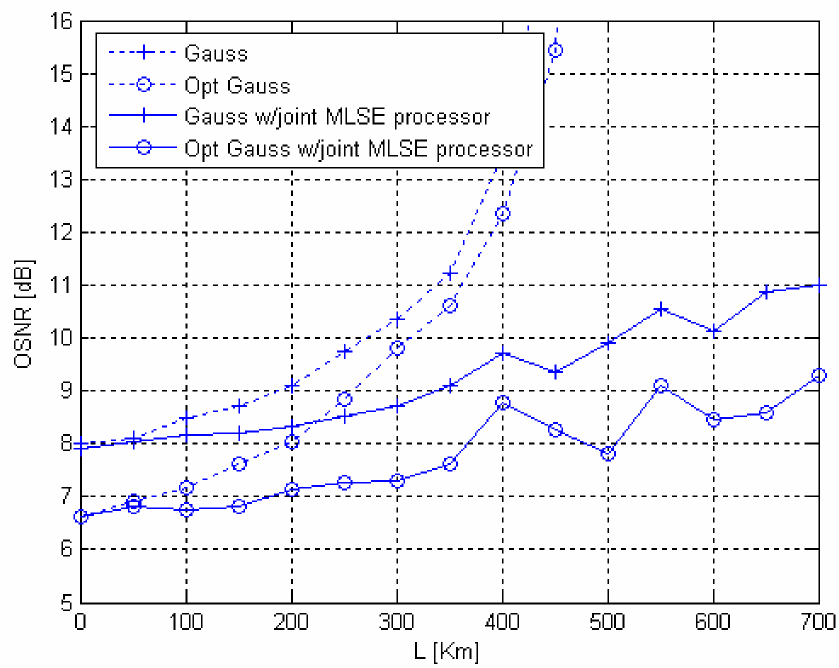


Figure 5.24. Performance of DQPSK system with joint 4-states MLSE processor

- **Use of a 2 bit/symbol 8-states parallel MLSE processor**

The system considered is the same than in the previous section, but replacing the joint MLSE processor with 4 states, with a joint MLSE processor that uses an 8 state trellis, which corresponds to a binary MLSE processor with $8^2$=64 states.

First, the bandwidths of the optical and electrical filters were set to 50 GHz and 7.5 GHz respectively. Then, the optimization of the bandwidths was done at a distance of 600 Km obtaining an optimum optical bandwidth equal to 6 GHz and an optimum electrical bandwidth equal to 14 GHz. The results are shown in Figure 5.25.

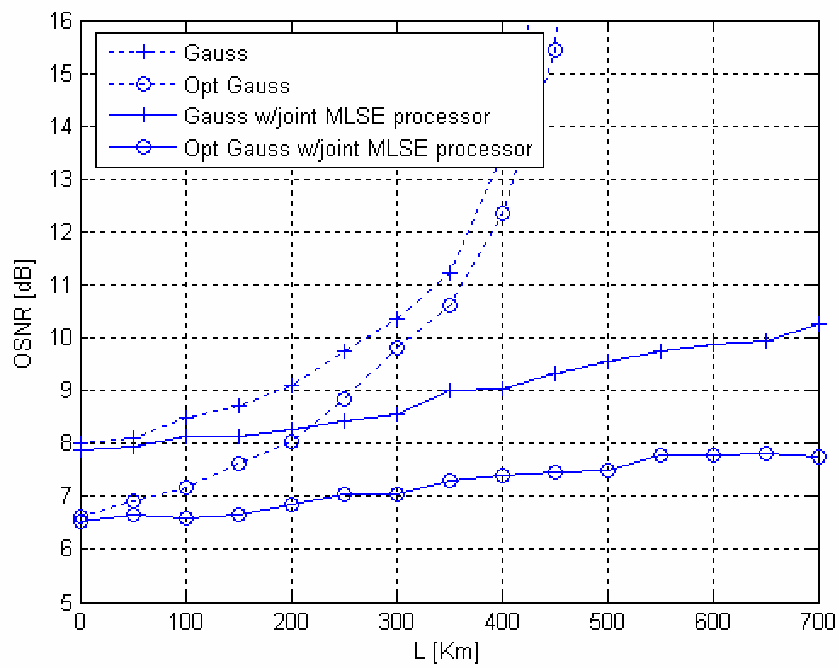


Figure 5.25. Performance of DQPSK system with joint 8-states MLSE processor

Results shown in Figure 5.25 confirm that a 2 bit/symbol 8-states parallel MLSE processor is very effective, as its use combined with filter optimization allows reaching 700 Km experiencing only less than 1.5 dB penalty with respect to the back to back performance (which requires an OSNR equal to 6.5 dB).

# Chapter 6

# Performance of the MLSE equalization in an optical communication system using a realistic fiber

In this chapter the results of a study done about how the use of MLSE receivers could improve the performance of IMDD, Duobinary, DPSK and DQPSK optical communications systems in the presence of both dispersion and non-linear effects are shown.

Two kinds of fiber are studied, first a standard Single Mode Fiber (SMF), and then a Non-Zero Dispersion Shifted Fiber (NZ-DSF).

The simulations of the optical system were done using the software Optsim, and the MLSE processor was implemented using Matlab.

## 6.1 System characteristics

The characteristics of the system set-up and simulation procedures are the following:

- The bit-rate is $R_b$ 10 Gbit/s.

- The Pseudo-Random Bit Sequence is PSRB = $2^{16} - 1$ = 65535 bits.
- Each bit is simulated using 20 samples.
- For DB, DPSK and DQPSK modulations the PRBS is properly precoded.
- The channel is formed by a single span of :
  - Single mode fiber with:

    $\alpha$ = 0.25 dB/Km

    D = 16 ps/nm/Km

    $\gamma$ = 1.3 1/W/Km
  - NZ-DSF with:

    $\alpha$ = 0.25 dB/Km

    D = 3.8 ps/nm/Km

    $\gamma$ = 1.5 1/W/Km
- After the fiber a EDFA amplifier with:

  G = 30 dB

  F = 6 dB

  is used, which completely recovers the losses introduced by the optical channel.
- The ASE noise is introduced by the amplifier.
- The receiver is assumed noiseless.
- The receiver is composed by a second order Supergaussian optical filter with bandwidth $B_o$, followed by an ideal photodetector and a fifth order Bessel electrical filter with bandwidth $B_e$. For the DPSK and DQPSK systems between the optical filter and the photodetector there is a 1-bit-delay Asymmetric Mach-Zehnder Interferometer.
- At the receiver's end 4, samples per bit are taken.
- For IMDD and DB the receiver is followed by a 32-states Viterbi MLSE processor. For DPSK a 32-states Viterbi MLSE processor is inserted in branch of the receiver, so the two signal samples are processed separately. For DQPSK a 2 bit/symbol 8-states parallel Viterbi MLSE processor is used.

- No optimization of the sampling instant is done at the receiver.
- For IMDD and DB, 2 samples per bit are used for the branch metric evaluation. For DPSK and DQPSK, 4 samples per bit are used instead, being more sensitive than IMDD and DB to the sampling instant within the bit slot.
- The system performance is measured according to the OSNR necessary to reach a BER value equal to $10^{-3}$, which ensures the operation below the FEC threshold.
- Simulations: Using an optical simulator we obtained the filtered electrical signal for various values of transmitted power (Ptx) and L (up to a maximum of Ptx equal to 20 dBm). For each value of Ptx, the corresponding value of OSNR was found using the expression:

$$OSNR_{db} = Ptx - \alpha L - F_{db} - 10\log(hfR_b) \quad (6.1)$$

where $h$ is the Plank constant and $f$ is the frequency.

Then, for each value of OSNR and L the Rx signal was processed by the MLSE, searching for the OSNR yielding the target performance of BER equal to $1.10^{-3}$.

## 6.2 Use of a standard single mode fiber

### 6.2.1 IMDD-NRZ modulation

The system set-up is shown in Figure 6.1. In this system the optimum filters found in section 5 were used, so the optical and electrical filters were set to 9 GHz and 24 GHz respectively, and the sqrt metric was applied by the MLSE processor.

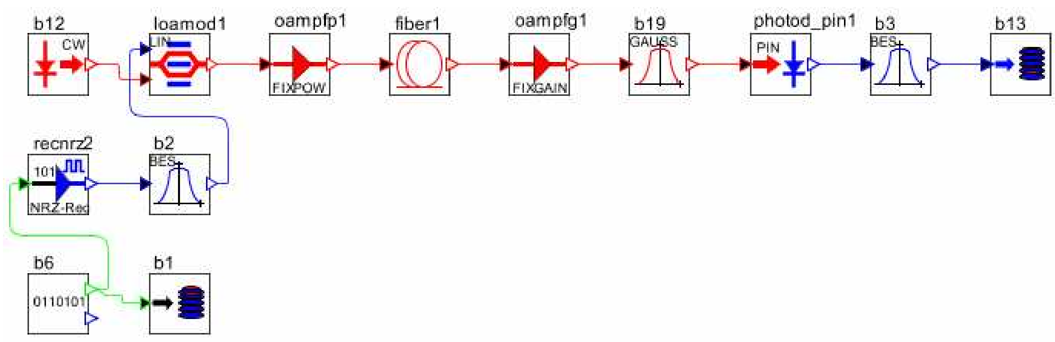


Figure 6.1. IMDD system using standard SMF fiber

The performance of the system is shown in Figure 6.2.

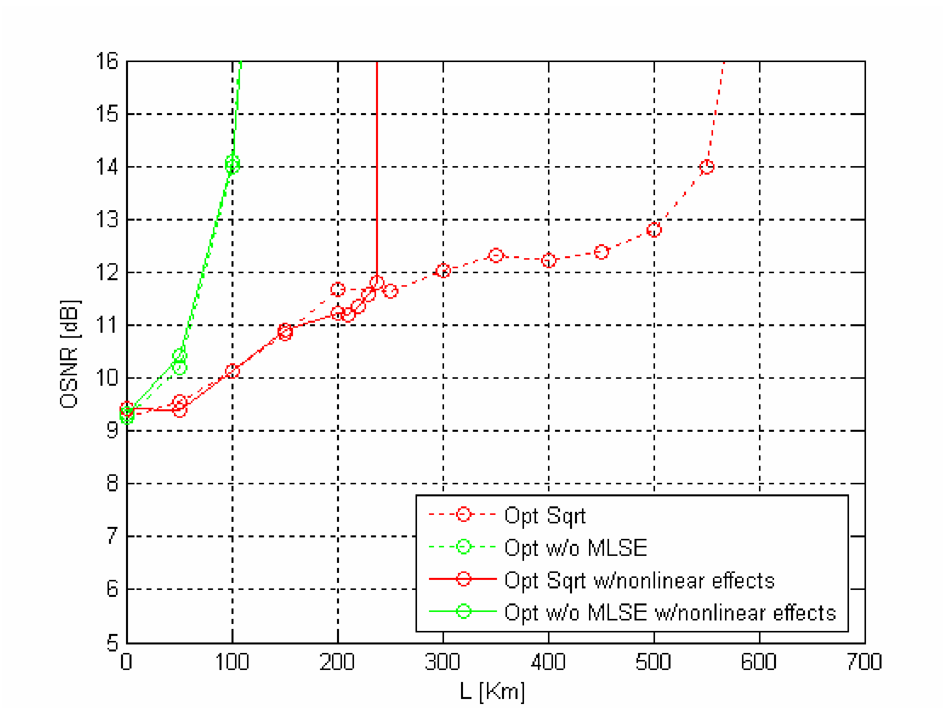


Figure 6.2. IMDD system with standard SMF vs IMDD system with dispersive fiber

The system is not limited by dispersion anymore; this time it is limited by the non linear effects, meaning the MLSE is not so effective in improving the performance of a system affected by non linear effects as well as dispersion as it is for a system affected just by dispersion. The consequence is that the maximum reachable distance is visibly reduced.

The maximum distance that can be reached is 238 Km, which corresponds to a value of OSNR equal to 12 dB, which is 62 Km less than the distance reached for the same value of OSNR when using purely dispersive fiber.

## 6.2.2 Duobinary modulation

The system set-up is shown in Figure 6.3. In this system the optimum filters found in section 5 were used, so the optical and electrical filters were set to 8 GHz and 29 GHz respectively, and the sqrt metric was applied at the MLSE processor.

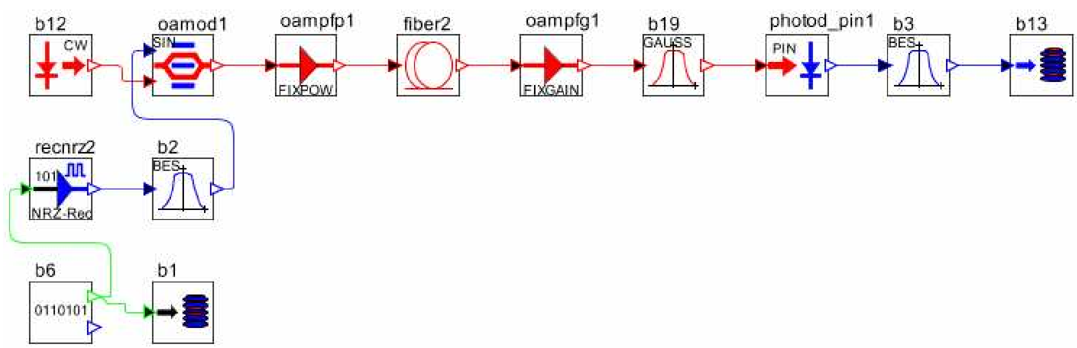


Figure 6.3. Duobinary system using standard SMF fiber

The performance of the system is shown in Figure 6.4. It can be observed that the maximum reachable distance is visibly reduced. So now the system is limited by the non linear effects instead of dispersion as it was before. The maximum reachable distance for the system affected by both dispersion and non linear effects is 242 Km for an OSNR value of 12 dB, while the system affected only by dispersion reaches a distance of 660 Km for the same OSNR value.

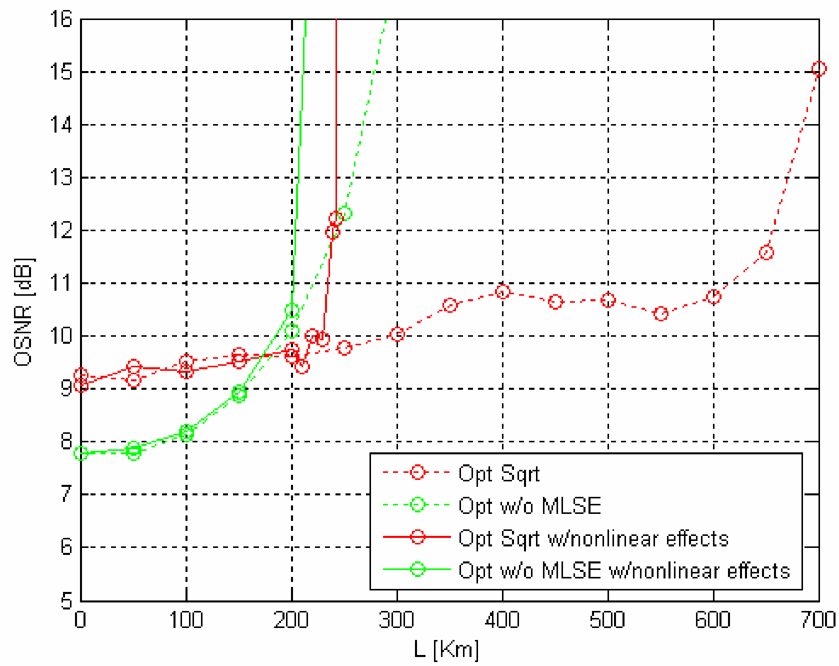


Figure 6.4. Duobinary system with standard SMF vs Duobinary system with dispersive fiber

### 6.2.3 DPSK modulation

The system set-up is shown in Figure 6.5. In this system the optimum filters found in section 5 were used, so the optical and electrical filters were set to 14 GHz and 22 GHz respectively, and the Gaussian metric was applied by the MLSE processor.

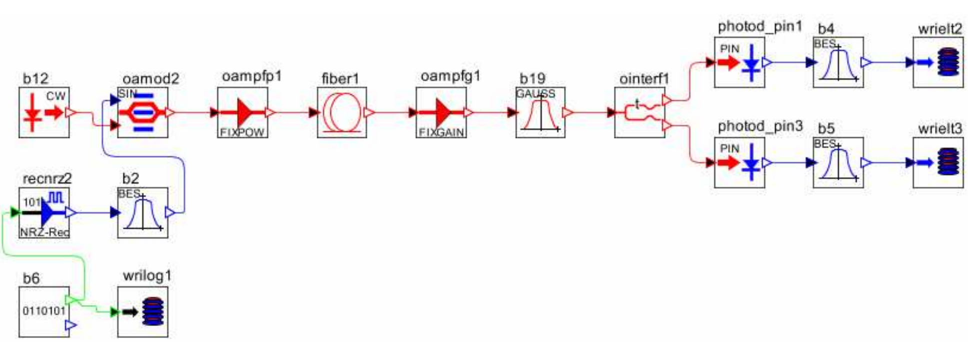


Figure 6.5. DPSK system using standard SMF fiber

The performance of the system is shown in Figure 6.6.

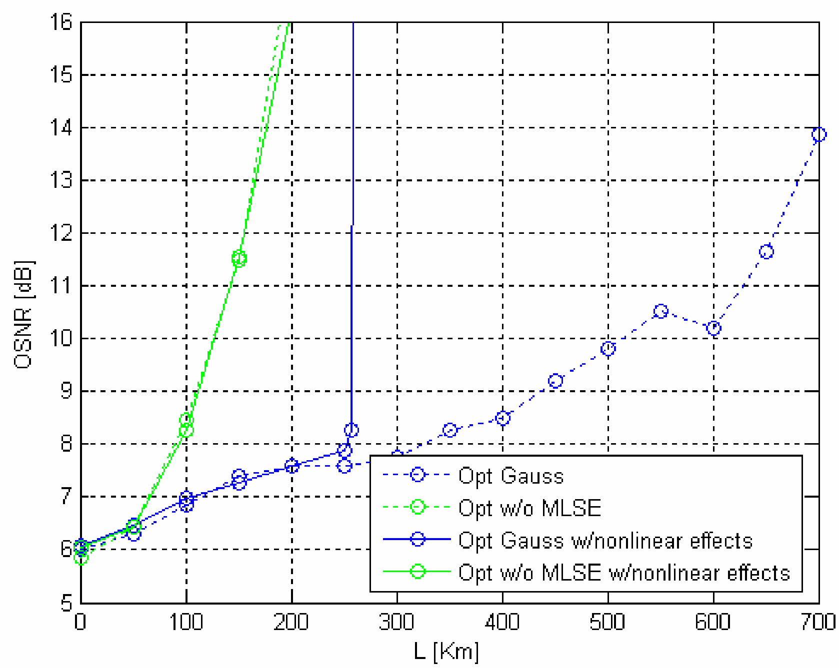


Figure 6.6. DPSK system with standard SMF vs DPSK system with dispersive fiber

It can be observed that the maximum reachable distance for the system affected by both dispersion and non linear effects is 258 Km for an OSNR value of 8 dB, while the system affected only by dispersion reaches a distance of 330 Km for the same OSNR value.

## 6.2.4 DQPSK modulation

The system set-up is shown in Figure 6.7. In this system the optimum filters found in section 5 were used so the optical and electrical filters were set to 6 GHz and 14 GHz respectively, and the Gaussian metric was applied by the MLSE processor.

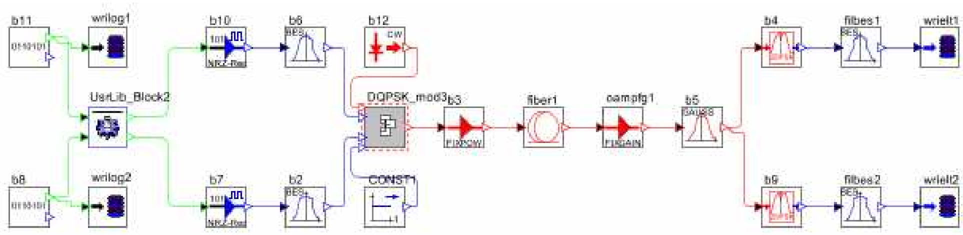


Figure 6.7. DQPSK system using standard SMF fiber

The performance of the system is shown in Figure 6.8.

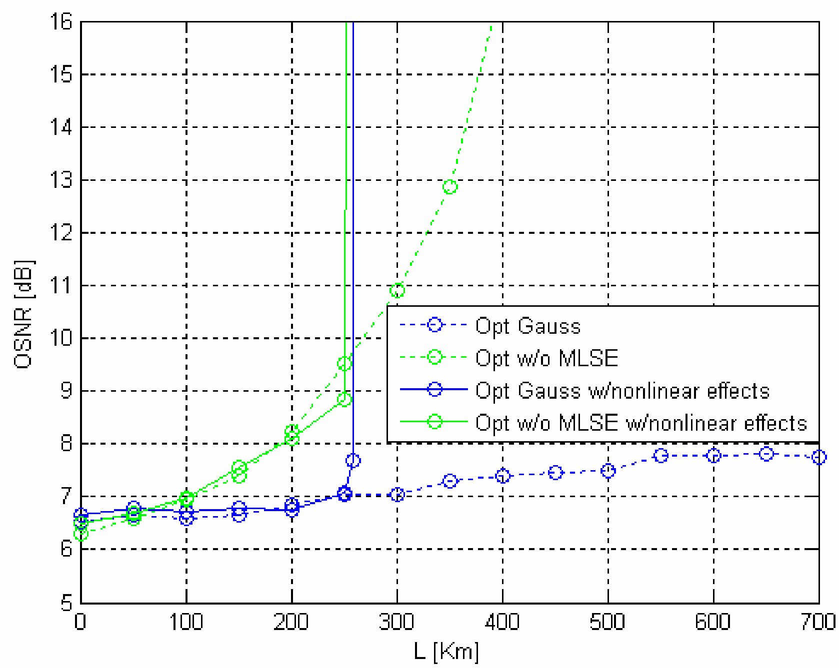


Figure 6.8. DQPSK system with standard SMF vs DQPSK system with dispersive fiber

It is seen that the maximum reachable distance for the system affected by both dispersion and non linear effects is 259 Km for an OSNR value of 7.7 dB, while the system affected only by dispersion reaches a distance of 700 Km for the same OSNR value.

## 6.3 Use of a non-zero dispersion shifted fiber

### 6.3.1 IMDD-NRZ modulation

The performance of the system is shown in Figure 6.9.

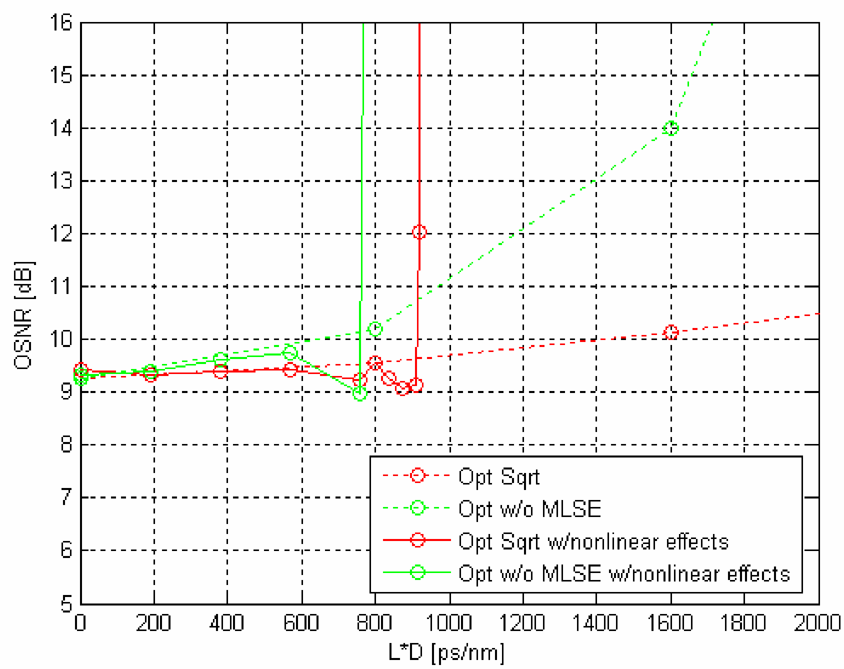


Figure 6.9. IMDD system with NZ-DSF vs IMDD system with dispersive fiber

It can be observed that the maximum reachable distance for the system affected by both dispersion and non linear effects is 247 Km for an OSNR value of 12 dB (which is 5 Km more than achieved when using a standard SMF), while the system affected only by dispersion reaches a distance of 300 Km for the same OSNR value.

## 6.3.2 Duobinary modulation

The performance of the system is shown in Figure 6.10.

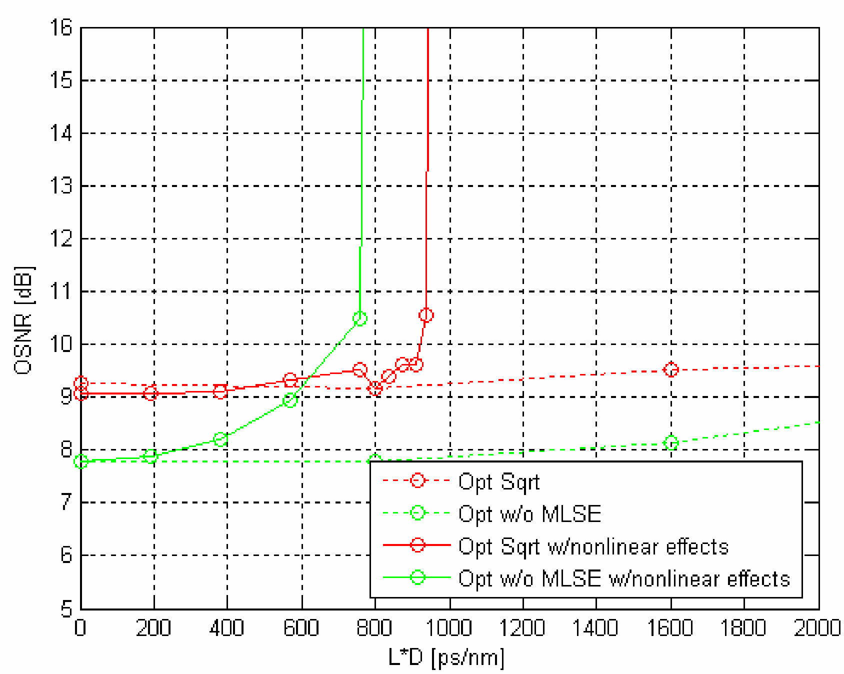


Figure 6.10. Duobinary system with NZ-DSF vs Duobinary system with dispersive fiber

It can be observed that the maximum reachable distance for the system affected by both dispersion and non linear effects is 247 Km (which is 4 Km more than achieved when using a standard SMF) for an OSNR value of 10.5 dB, while the system affected only by dispersion reaches a distance of 340 Km for the same OSNR value.

## 6.3.3 DPSK modulation

The performance of the system is shown in Figure 6.11.

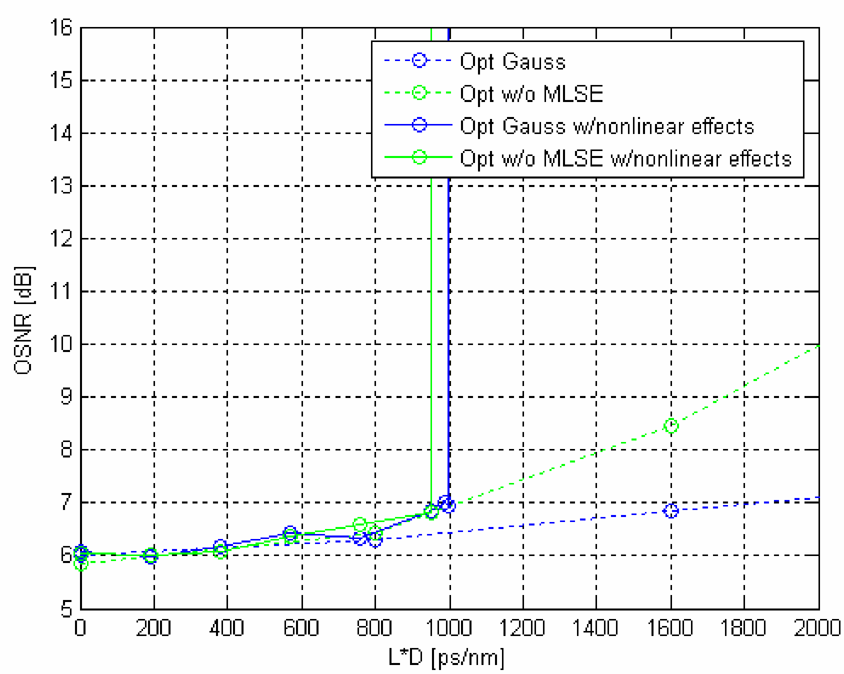


Figure 6.11. DPSK system with NZ-DSF vs DPSK system with dispersive fiber

It can be observed that the maximum reachable distance for the system affected by both dispersion and non linear effects is 262 Km (which is 4 Km more than achieved when using a standard SMF) for an OSNR value of 7 dB, while the system affected only by dispersion reaches a distance of 470 Km for the same OSNR value.

### 6.3.4 DQPSK modulation

The performance of the system is shown in Figure 6.12.

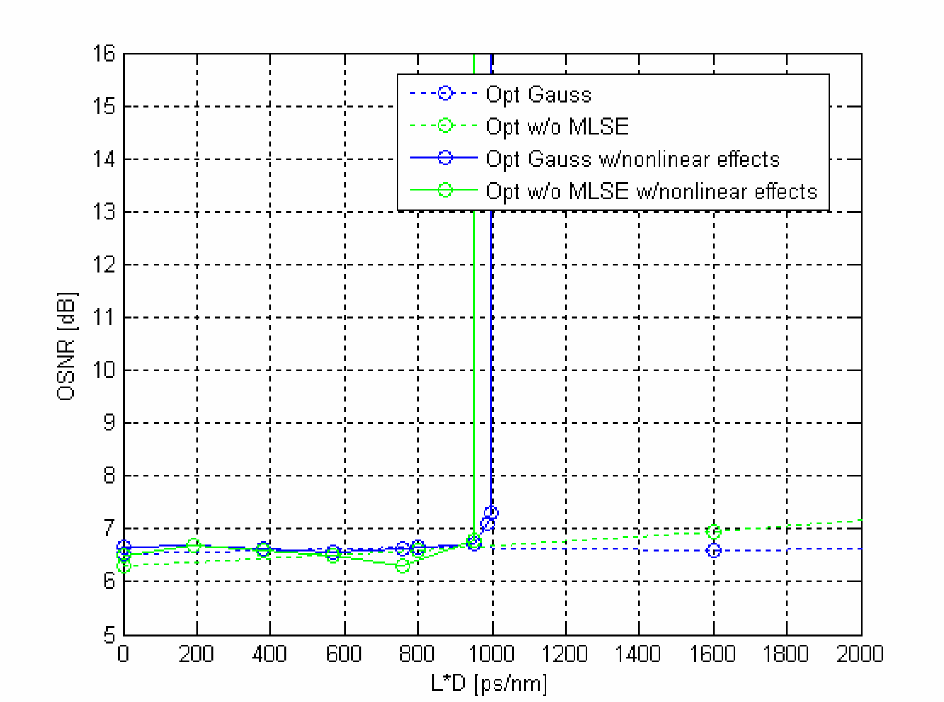


Figure 6.12. DQPSK system with NZ-DSF vs DQPSK system with dispersive fiber

It can be observed that the maximum reachable distance for the system affected by both dispersion and non linear effects is 262 Km (which is 3 Km more than achieved when using a standard SMF) for an OSNR value of 7.3 dB, while the system affected only by dispersion reaches a distance of 400 Km for the same OSNR value.

# Conclusions

From its beginnings on, optical communications systems have adopted the IMDD modulation. Nevertheless, it has been shown that the use of other alternative modulation schemes such as DB, DPSK and DQPSK can be effective in mitigating the phenomenon of dispersion, allowing the reaching of higher distances. For the system analyzed in this work, it has been shown that for an OSNR equal to 12 dB (OSNR necessary to reach a BER of $1.10^{-3}$) we can go from 40 Km for the IMDD modulation to 115 Km using the DPSK modulation and to 275 using the DQPSK modulation. DB does not yield such good results in this case since it causes the OSNR to stay above 12 dB.

In this study it has also been demonstrated that the simultaneous use of filters optimization techniques and of alternative modulations formats achieves even better results. In fact,  from 75 Km achieved for the IMDD modulation, we can go to 245 Km using the DB modulation, to 190 Km using the DPSK modulation and to 295 Km using the DQPSK modulation. It is important to point out the fact that for DB modulation, the optimization of the filters appears to be really effective.

Yet, the most promising technique to fight dispersion is the use of MLSE equalization in the receiver.

In this study it has been demonstrated that the simultaneous use of the optimal filters and a 32-states MLSE equalizer which uses the Viterbi algorithm with Gaussian metric, a distance of 200 Km can be reached using the IMDD modulation;

650 Km using DB modulation; 590 Km using the DPSK modulation and 390 using the DQPSK modulation. It can be observed that the DQPSK modulation does not benefit from the MLSE equalization, not even in the case of using optimal filters.

In order to improve the performance of the systems using IMDD and DB modulations, the use of the sqrt metric for the branch metric evaluation was introduced, instead of the Gaussian metric. By doing so, the distance reached for the IMDD system was extended by 100 Km, reaching then 300 Km; while the DB system does from 335 Km to 610 Km for an OSNR equal to 11 dB, and reaches 655 Km for an OSNR equal to 12 dB. It was verified that for the DPSK and DQPSK modulations the sqrt metric does not give any performance improvement.

In turn, the system using DPSK modulation was improved by performing the MLSE equalization in each branch of the receiver, rather than inserting the MLSE processor right after the balanced receiver. By doing so, a distance of 680 Km was reached.

The system using the DQPSK modulation was improved by using a 2 bit/symbol parallel MLSE processor. Using a 32-states processor 700 Km were reached with an OSNR equal to 9.3 dB, and using a 64-states processor 700 Km were reached with an OSNR lower than 8dB.

Experiments carried out show that for any modulation scheme, when using an MLSE processor, the performance of the systems is significantly improved when the number of states of the processor increases. Nevertheless, the performance improvement and the increase of computational complexity reached when the number of states is increased must be weighed, and we believe that a number of states equal to 32 allows for a good balance.

Using a standard SMF fiber, the maximum distance that can be reached is limited by the non-linear effects. Even when using the optimal filters and the optimal configuration of the MLSE processor, this distance is reduced to 235 Km for the systems using the IMDD and DB modulations, to 255 for the system using the PSK modulation and to 260 Km for the system using the DQPSK modulation.

The techniques here studied may be introduced in an optical communications system without touching the fiber already installed, and from the results here obtained, it may be observed that they are very effective in counteracting the effects produced by chromatic dispersion. This are characteristics which make them usable when upgrading the bit-rate of current systems, since they avoid making changes in the transmission channel and control the larger chromatic dispersion effects produced when increasing the bit-rate.

# References


[1] "A Brief History of Fiber Optical Technology" [online], *FI*. 2005. 22 Aug. 2007. <http://www.fiber-optics.info/fiber-history.htm>.

[2] "Types of Optical Fiber" [online], *FI*. 2005. 22 Aug. 2007. <http://www.fiber-optics.info/articles/fiber-types.htm>.

[3] A. Girard, "Polarization of Light in Fiber Causes Signal Dispersion", Canada, Exfo Electro-optical Engineering, 2000.

[4] I. Karminow and L. Tingye, "Optical fiber telecommunications IVB: systems and impairements", San Diego, Academic Press, 2002.

[5] N. Alic, G. C. Papen, R. E. Saperstein, L. B. Milstein and Y. Fainman, "Signal statistics and maximum likelihood sequence estimation in intensity modulated fiber optic links containing a single optical preamplifier", Opt. Exp., Vol. 13, issue 5, pp. 4568-4579, Jun 2005.

[6] G. Bosco, P. Poggiolini and M. Visintin, "Performance Analysis of MLSE Receivers Based on the Square Root Metric", *ECOC 2007*, Berlin, Germany, 16-20 Sep. 2007.

[7] S. Benedetto and E. Biglieri, "Principles of Digital Transmission: with wireless application", New York, Klumer Academic Publishers, 1999.

# Bibliography

O. E. Agazzi, M. R. Hueda, H. S. Carrer and D. E. Crivelli, “Maximum Likelihood Sequence Estimation in Dispersive Optical Channels”, *IEEE Journal of Lightwave Technology,* ISBN: 0733-8724, Vol. 23, pp 749–763, Feb. 2005.

G. P. Agrawal, “Fiber-optic communications systems”, Rochester, NY, Wiley Interscience, 2002.

N. Alic, G. C. Papen and Y. Fainman, “Theoretical Performance Analysis of Maximum Likelihood Sequence Estimation in Intensity Modulated Short-Haul Fiber Optic Links”, *Lasers and Electro-Optics Society LEOS,* 2004.

S. Aramideh, “Advanced Signal Processing Engines for Next Generation Optical Transport Systems” [online]. *Fiber Optic Technology*. April 2005. 22 Aug. 2007. <http://www.coreoptics.com/news/press_archiv_2005.php>.

F. Audet, “Dispersion-compensation fiber: precision and repetition”, Canada, Exfo Electro-optical Engineering, 2000.

G. Bosco and P. Poggiolini, “Long-distance Effectiveness of MLSE IMDD Receivers”, *IEEE Photonics Technology Letters*, Vol. 18, Issue 9, pp. 1037–1039, May 2006.

M. Cavallari, C.R.S. Fludger and P.J. Anslow, “Electronic Signal Processing for Differential Phase Modulation Formats”, *Optical Fiber Communication Conference, 2004. OFC 2004* Vol. 1, 23 Feb. 2004.

J. Crisp, “Introduction to fiber optics”, Oxford, Newnes, 1996.

J. Downie, M. Sauer and J. Hurley, “Experimental measurements of uncompensated reach increase from MLSE-EDC with regard to measurement BER and modulation format”, *Optics Express*, Vol. 14, Issue 24, pp. 11520-11527.

J. P. Elbers, H. Wernz, H. Griesser, C. Glingener, A. Faerbert, S. Langenbach, N. Stojanovic, C. Dorschky, T. Kupfer, and C. Schulien, "Measurement of the dispersion tolerance of Optical Duobinary with an MLSE-Receiver at 10.7 Gb/s," *Optical Fiber Communication Conference and Exhibition* and *The National Fiber Optic Engineers Conference*, Optical Society of America, Washington, D.C., 2005.

L. E. Frenzel, “100-Gbit Networks On The Horizon” [online]. *Electronic Desing*. July 2007. 22 Aug. 2007. <http://electronicdesign.com/Articles/Index.cfm?ArticleID=15995>.

L. E. Frenzel, “Happy days are here again for fiber-optical communications” [online]. *Electronic desing*. May 2007. 22 Aug. 2007. <http://electronicdesign.com/Articles/Index.cfm?ArticleID=15630>.

R. Gaudino and P. Poggiolini, “Reti in fibra ottica”, Torino, Politeko, 2005.

G. Goldfarb and G. Li, “Coherent optial communications via digital signal processing” [online]. *SPIE*. January 2007. 22 Aug. 2007. <http://spie.org/x16081.xml>.

G. Grano,“Utilizzo della ricezione a massima verosimiglianza (MLSE) nelle comunicazioni ottiche”, (Thesis), Torino: Politecnico di Torino, 2006.

M. R. Hueda, D. E. Crivelli, H. S.Carrer and O. E. Agazzi, “On the Performance of Reduced-State Viterbi Receivers in IM/DD Optical Transmission Systems”, *European Conference on Optical Communication (ECOC 2004)*, Stockholm, Sweden, September 2004.

L. Kazovsky, S Benedetto and A, Willner, “Optical fiber communication systems”, Boston-London, Artech House, 1996.

P. Poggiolini, G. Bosco, J. Prat, R. Killey and S. Savory, “1,040 km uncompensated IMDD transmission over G.652 fiber at 10 Gbit/s using a reduced- state SQRT-metric MLSE receiver", *ECOC 2006*, Post-Deadline Paper Th4.4.6, Cannes, France, 24-28 Sep. 2006.

P. Poggiolini, G. Bosco, J. Prat, R. Killey and S. Savory, "Branch Metrics for Effective Long-Haul MLSE IMDD Receivers", *ECOC 2006*, Paper We2.5.4, Cannes, France, 24-28 Sep. 2006.

J. G. Proakis, "Digital communications", Boston, McGraw-Hill, 2001.

T. S. Rappaport, "Wireless Communications: principles and practice", New Jersey, Prentice Hall, 2002.

H. Shankar, "Duobinary Modulation For Optical Systems" [online]. *INPHI*. 7 Feb 2002. 22 Aug. 2007. <http://www.inphi-corp.com/products/whitepapers/DuobinaryModulationForOpticalSystems.pdf>.

A. Singh, "Modulation Formats for High-Speed, Long-Haul Fiber Optic Communication Systems" [online]. *INPHI*. 7 Feb. 2002. 9 Oct. 2007. <http://www.inphi-corp.com/products/whitepapers/RZNRZ_final.pdf>.

C. Xia and W. Rosenkranz, "Electrical dispersion compensation for different modulation formats with optical filtering", *Optical Fiber Communication Conference 2006* and *the 2006 National Fiber Optic Engineers Conference. OFC 2006*, 5 March 2006.

"History of fiber optics" [online]. *Timbercon*. 22 Aug. 2007. <http://www.timbercon.com/History-of-Fiber-Optics/index.html>.

"The Effects of Dispersion on High-speed Fiber Optic Data Transmission" [online]. *FI*. 2005. 22 Aug. 2007. <http://www.fiber-optics.info/articles/dispersion.htm>.